Pion-nucleus double charge exchange and the nuclear shell model

N. Auerbach,* W. R. Gibbs, and Joseph N. Ginocchio
Theoretical Division, Los Alamos National Laboratory, Los Alamos, New Mexico 87545

W. B. Kaufmann
Department of Physics, Arizona State University, Tempe, Arizona 85287
(Received 29 March 1988)

The pion-nucleus double charge exchange reaction is studied with special emphasis on nuclear structure. The reaction mechanism and nuclear structure aspects of the process are separated using both the plane-wave and distorted-wave impulse approximations. Predictions are made employing both the seniority model and a full shell model (with a single active orbit). Transitions to the double analog state and to the ground state of the residual nucleus are computed. The seniority model yields particularly simple relations among double charge exchange cross sections for nuclei within the same shell. Limitations of the seniority model and of the plane-wave impulse approximation are discussed as well as extensions to the generalized seniority scheme. Applications of the foregoing ideas to single charge exchange are also presented.

I. INTRODUCTION

The double charge exchange (DCX) reaction has held out the hope for many years that it would be a means of probing the short-range part of the nucleon-nucleon correlations in the nucleus. In order to realize this goal, one must confront the data with calculations which include various degrees of correlations. In early calculations it was found that uncorrelated nuclear wave functions gave qualitative agreement with experiment at the highest energies ($\sim$300 MeV) and considerable disagreement in the resonance region ($\sim$160 MeV).[1] More recently it was found that, at low energies ($\sim$50 MeV), the disagreement was very large (approximately a factor of 50)[2] with the uncorrelated wave functions, while theories including correlation effects come much closer to the data.[3,4]

Aside from comparison with the absolute magnitude discussed above, it is also possible to compare the DCX reactions on various nuclides in the same shell, one of the simplest cases being ^{42}Ca-^{44}Ca-^{48}Ca. If the reaction proceeds by a long-range process then all excess neutron pairs will take part, and the cross section is expected to be proportional to the total number of such neutron pairs, giving a ratio of 1:6:28 for the three isotopes given above. These ratios had previously been observed[5] to be violated at resonance energies, and a recent experiment[6] at 35 MeV found the ratio ^{44}Ca/^{42}Ca to be about $\frac{1}{2}$ instead of the 6 predicted by the uncorrelated picture.

In order to obtain a more detailed picture of the physics one needs to compare a number of nuclides throughout a shell. The data should be compared with a many-body solution or a full shell-model calculation. However, there are simplified versions of the shell model such as the seniority scheme[7] which have proved quite successful in providing expressions for the energy levels[8] and neutron radii.[9] We will show (following Ref. 10) that the DCX amplitude can be written as the sum of two amplitudes in this model. The first amplitude favors the long-range process and has the property that the cross sections due to it alone obey the excess-neutron-pair rule discussed above. The second amplitude corresponds to a shorter internucleon range, and its dependence on the number of excess neutrons is different but can still be expressed simply. [See Eqs. (4.4)–(4.6).]

Since there are two complex amplitudes and the overall phase is not measurable, there are only three independent quantities, and the measurement of four (or more) cross sections in a given shell provides a test of the seniority model without specifying the reaction mechanism (except that the operator must have a purely two-body nature). The statements just made assume that all of the reactions have the same Q value and that distortion of the pion waves remains constant throughout the shell. Since this is not true in practice, corrections for these effects must be made, and experiments which minimize them are to be preferred.

Beyond the test of the nuclear wave functions mentioned above, the reaction operator itself is also of interest for two reasons. First, one needs to know the region of contribution of the "short-range" amplitude so that it is known at what internucleon distances the nuclear wave functions are being tested. The citation of this distance provides a figure of merit for the wave-function test. Second, if the range is very short, as is shown in Sec. VI for the simple model of sequential exchanges, then one is led to consider alternatives to this simple process usually calculated.[11–13]

We note that the uncorrelated model introduced at the first of this section has served us well in showing that correlations are needed. The hope is that deviations from the present work on shell-model correlations will provide evidence for short-range correlations beyond those of the shell model.

The article is arranged as follows. General properties of the DCX operator in the shell model are studied in

Sec. II. The matrix element of a general two-nucleon operator in the seniority model with isospin is evaluated in Sec. III. It is shown that there are at most three independent reduced matrix elements and, for nonisoscalar operators, only two. Thus the model places powerful constraints on matrix elements within a shell. For complex scattering amplitudes, five independent measurements suffice to determine an isoscalar operator, and only three are needed for a nonisoscalar operator. (The overall phase is unobservable.) The model is applied to the isotensor ($T=2$) DCX operator in Sec. IV. As a specific example the $f_{7/2}$ shell is examined, and relationships among DCX reactions to both analog and ground states are derived.

Within the $f_{7/2}$ shell-model space, the seniority model is valid for nuclei with valence particles or holes of one kind, for example, the calcium isotopes. However, for nuclei with both valence neutrons and protons active, seniority is not conserved.[14] In Sec. V a more realistic $f_{7/2}$ shell model is considered. Section VI is devoted to reaction model calculations of the independent matrix elements for the case of the $f_{7/2}$ shell. In Sec. VII this model is used to calculate DCX cross sections for both the seniority model and the realistic model both of which are compared to existing data. The calculations, performed in the plane wave impulse approximation (PWIA) (appropriate to low-energy pions only) and the distorted-wave impulse approximation (DWIA), reproduce qualitatively the DCX cross sections on the Ca isotopes for $T_\pi < 70$ MeV.

Section VIII shows that similar considerations can be applied to single charge exchange. Section IX carries the ideas presented in the earlier parts of the paper to the generalized seniority model, where more than a single shell is involved.

II. THE DCX OPERATOR IN THE SHELL MODEL

The double charge exchange operator F is, in lowest order, a two-nucleon operator. In this paper we shall ignore the three-nucleon, etc., contributions and assume that it is indeed a two-nucleon operator. Since it changes two neutrons (protons) into two protons (neutrons) F is an isotensor operator. The second-order processes considered in F will also contribute to both elastic and inelastic scattering as well as single charge exchange. However, in those reactions the lowest-order operator is a one-nucleon operator which in general will dominate over the second-order processes. In fact it is for this reason that the DCX is a unique probe in nuclear physics.

The DCX operator will be a function of the coordinates $\mathbf{r}_1, \mathbf{r}_2$, spin variables σ_1, σ_2, and the isospin variables $\hat{\mathbf{T}}_-(1), \hat{\mathbf{T}}_-(2)$ of the two nucleons. A sufficiently general form of the DCX operator which includes both the sequential single charge exchange and the meson exchange mechanisms between 0^+ states will be

$$F_{12}(\mathbf{k},\mathbf{k}') = [\mathcal{J}_0(\mathbf{r}_1,\mathbf{r}_2) + \mathcal{J}_1(\mathbf{r}_1,\mathbf{r}_2)\boldsymbol{\sigma}_1\cdot\hat{\mathbf{e}}_1\boldsymbol{\sigma}_2\cdot\hat{\mathbf{e}}_2] \times \hat{\mathbf{T}}_-(1)\hat{\mathbf{T}}_-(2) , \tag{2.1}$$

where $\hat{\mathbf{e}}_{1,2}$ are model-specific unit vectors, $\mathbf{k},\mathbf{k}'$ are the initial and final pion momenta, and $\cdot$ means scalar product. The $\mathcal{J}_{0,1}$ are complex scattering amplitudes. Within the shell-model space, we need only the matrix elements of this operator with respect to the wave functions of two nucleons in the valence shell.

The many-nucleon matrix elements of the operator are then determined by the two-nucleon density of the many-nucleon wave functions; these matrix elements will be derived in Secs. III–V. For this purpose it is convenient to express the operator (2.1) in terms of the operators $a^\dagger_{jm}, b^\dagger_{jm}$ ($\tilde{a}_{jm}, \tilde{b}_{jm}$) which create (destroy) a valence neutron and proton, respectively, in the spherical valence shell-model orbital with single-nucleon angular momentum j and projection m. For $0^+ \to 0^+$ transitions the DCX operator in the multipole form is

$$F = \Omega \sum_L F_L(\mathbf{k},\mathbf{k}')(b^\dagger_j \tilde{a}_j)^{(L)}(b^\dagger_j \tilde{a}_j)^{(L)}/(2L+1) , \tag{2.2}$$

where $\Omega = j + \frac{1}{2}$, and $(\ )^L$ means coupled to angular momentum rank L. The complex amplitudes F_L for even L involve only the spin-independent $\mathcal{J}_0$:

$$F_L = G^{Llj} \int d^3r_1\, d^3r_2\, \mathcal{J}_0(\mathbf{r}_1,\mathbf{r}_2) Y_L(\hat{\mathbf{r}}_1)\cdot Y_L(\hat{\mathbf{r}}_2) \rho_{nlj}(r_1,r_2), \quad L \text{ even} , \tag{2.3a}$$

where

$$G^{Llj} = \frac{(2l+1)^2(2j+1)}{4\pi} \left[\begin{Bmatrix} L & l & l \\ \frac{1}{2} & j & j \end{Bmatrix} \begin{pmatrix} l & l & L \\ 0 & 0 & 0 \end{pmatrix} \right]^2 , \tag{2.3b}$$

$$\rho_{nlj}(r_1,r_2) = \Psi^{(\pi)}_{nlj}(r_1)\Psi^{(\pi)}_{nlj}(r_2)\Psi^{(\nu)}_{nlj}(r_1)\Psi^{(\nu)}_{nlj}(r_2) . \tag{2.3c}$$

The single-neutron (proton) radial wave functions are $\Psi^{(\nu)}_{nlj}(r)$ [$\Psi^{(\pi)}_{nlj}(r)$] with orbital angular momentum l and radial quantum number n, the $Y_{lm}(\hat{\mathbf{r}})$ are spherical harmonics, and $\{\ \}$ and $(\ )$ are six-j and three-j symbols, respectively. The complex amplitude for L odd involves only the spin-dependent $\mathcal{J}_1$:

$$F_L = \Sigma_{\lambda\lambda'} D_{\lambda Llj} D_{\lambda' Llj} \times \int d^3r_1\, d^3r_2\, \mathcal{J}_1(r_1,r_2) Y_{\lambda L}(\hat{\mathbf{r}}_1)\cdot Y_{\lambda' L}(\hat{\mathbf{r}}_2) \rho_{nlj}(r_1,r_2) , \quad L \text{ odd} , \tag{2.4a}$$

where

$$D_{\lambda Llj} = \begin{Bmatrix} \lambda & 1 & L \\ l & \frac{1}{2} & j \\ l & \frac{1}{2} & j \end{Bmatrix} \begin{pmatrix} l & l & \lambda \\ 0 & 0 & 0 \end{pmatrix} \times \sqrt{2(2j+1)(2\lambda+1)}(2l+1) \tag{2.4b}$$

and the $Y_{\lambda LM}$ is the vector spherical harmonic

$$Y_{\lambda LM}(\hat{\mathbf{r}}_1) = [Y_\lambda(\hat{\mathbf{r}}_1) Y_1(\hat{\mathbf{e}}_1)]^{(L)}_M . \tag{2.4c}$$

The coefficients $F_L(\mathbf{k},\mathbf{k}')$ depend on the pion-nucleon dynamics, the pion energy, and the single-nucleon wave functions. We treat the explicit evaluation of the F_L in Sec. VI. For the present section we consider them to be complex parameters.

From (2.3) and (2.4) we see that, if the pion-nucleon interaction is spin independent, only the even multipoles

will contribute; if there is spin dependence the odd multipoles will also appear, $L=0,1,\ldots,2j$. However, these $2j+1$ complex amplitudes are not all independent. This can be seen by recoupling so that the pair of protons and pair of neutrons are each coupled to angular momentum J:

$$F=\sum_{J=0}^{2j-1} G_J(b_j^\dagger b_j^\dagger)^{(J)}\cdot(\tilde{a}_j\tilde{a}_j)^{(J)} , \tag{2.5a}$$

where

$$G_J=-\Omega\sum_L \begin{Bmatrix} j & j & L \\ j & j & J \end{Bmatrix} F_L . \tag{2.5b}$$

Because of the Pauli principle only even values of J are allowed, $J=0,2,\ldots,2j-1$, and hence there are really only $j+\frac{1}{2}$ independent complex amplitudes G_J. Furthermore, since the monopole operator is proportional to the isospin lowering operator $\hat{T}_-$,

$$\hat{T}_-=\sqrt{2\Omega}(b_j^\dagger\tilde{a}_j)^{(0)} , \tag{2.6}$$

the monopole part of the DCX operator is involved only in the double-analog charge exchange transition. Hence for non-double-analog charge exchange transitions there are only $j-\frac{1}{2}$ complex amplitudes. Therefore, for both spin-dependent and spin-independent transitions the number of independent amplitudes are the same, but of course their values depend on whether or not spin dependence is included.

For a single j shell there is a particle-hole symmetry in the double charge exchange reaction if other configurations are ignored and the mass dependence of the pion distorted waves and the nuclear mean field are neglected. Making the particle-hole transformation

$$a_{jm}^\dagger, b_{jm}^\dagger \rightarrow \tilde{\alpha}_{jm}, \tilde{\beta}_{jm} , \tag{2.7a}$$

$$\tilde{\alpha}_{jm}, \tilde{b}_{jm} \rightarrow -\alpha_{jm}^\dagger, -\beta_{jm}^\dagger , \tag{2.7b}$$

and using the anticommutation relations, the double charge exchange operator becomes

$$F\rightarrow\bar{F}=\Omega\sum_L F_L(\alpha_j^\dagger\tilde{\beta}_j)^{(L)}\cdot(\alpha_j^\dagger\tilde{\beta}_j)^{(L)} . \tag{2.8}$$

Hence we see that the double charge exchange on the target nucleus with n_π, n_ν valence neutrons and protons is the same as the target nucleus with $\bar{n}_\pi, \bar{n}_\nu$ valence neutrons and proton holes, where

$$\bar{n}_\pi=2\Omega-n_\pi , \tag{2.9a}$$

$$\bar{n}_\nu=2\Omega-n_\nu \tag{2.9b}$$

which is equivalent to changing the *total* number of valence nucleons ($n=n_\pi+n_\nu$) to holes and keeping the same isospin:

$$\bar{n}=4\Omega-n , \tag{2.10a}$$

$$\bar{T}=T . \tag{2.10b}$$

Of course this symmetry will not be exact because there will be mass dependence in the coefficients F_L from pion distortion and the shell-model radial wave functions. Also there can be admixtures of other configurations in the nuclear wave function. However, it would be of interest to do experiments on nuclear targets which are particle-hole conjugates, particularly for pion energies for which distortions are believed to be small and nuclear targets for which configuration admixtures are small. Even though this symmetry may be difficult to observe, it is useful for calculations since the nuclear structure matrix elements remain the same, only the F_L change.

III. THE SENIORITY MODEL

The seniority model has been extensively covered in the literature[7,15] we shall only briefly review the fundamental ideas in this section. The basic assumptions of the seniority model are (1) the dominant effective interaction between valence nucleons occurs for nucleons coupled to angular momentum zero and isospin one, and (2) the single-nucleon energies are degenerate or quasidegenerate. Assumption (1) is not good for nuclei which have both valence neutrons and protons active[14] as discussed in Sec. V. A generalized seniority model[16] has also been proposed which removes the assumption (2) and it shall be discussed in Sec. IX. In this section we shall deal with a single spherical shell with angular momentum j so the assumption (2) is valid. However, the results in this section also apply to the seniority model with degenerate single-nucleon energies.

The ground state of the seniority model wave function is composed entirely of $J^\pi=0^+$, $T=1$ pairs of nucleons outside a doubly magic core. These pairs are

$$S_1^\dagger=\tfrac{1}{2}\sum_m(-1)^{j-m}a_{jm}^\dagger a_{j-m}^\dagger , \tag{3.1a}$$

$$S_0^\dagger=\sqrt{\tfrac{1}{2}}\sum_m(-1)^{j-m}a_{jm}^\dagger b_{j-m}^\dagger , \tag{3.1b}$$

$$S_{-1}^\dagger=\tfrac{1}{2}\sum_m(-1)^{j-m}b_{jm}^\dagger b_{j-m}^\dagger . \tag{3.1c}$$

We shall also use a more compact isospin notation for which

$$c_{jm;\tau\mu}^\dagger=\begin{cases} a_{jm}^\dagger, & \mu=\frac{1}{2} \\ b_{jm}^\dagger, & \mu=-\frac{1}{2} \end{cases} , \tag{3.2a}$$

$$S_q^\dagger=\Omega(c_{j\tau}^\dagger c_{j\tau}^\dagger)_{0,q}^{J=0,T=1} \tag{3.2b}$$

where $(\ )_{M,T_z}^{J,T}$ means coupled to angular momentum J and projection M and isospin T and projection T_z.

These three pair creation operators $S_q^\dagger$ form an isospin triplet, where $q=-1,0,1$ is the isospin projection. For neutrons and protons outside the doubly magic core denoted by $|0\rangle$ the seniority-zero ground state is

$$|n,T,T_z,v=J=0\rangle=\eta(n,T)(S^\dagger\cdot S^\dagger)^{(n-2T)/4}\times(S^\dagger)^{T,T_z}|0\rangle , \tag{3.3}$$

where n is the number of valence nucleons outside the core and must be even for seniority zero and $\eta(n,T)$ is the normalization of the state. The core has isospin zero

and hence the isospin T is carried by the valence nucleons. The isospin projection is $T_z=(N-Z)/2$, where N is the total number of neutrons and Z is the total number of protons in the nucleus. The notation $(S^\dagger)^T_{T_z}$ means that T pairs are coupled to isospin T and projection T_z. For $T_z=T$, which is true for most targets, $(S^\dagger)^T_T=(S^\dagger_1)^T$, i.e., a product of all neutron pairs. The four-nucleon isoscalar product is

$$S^\dagger\cdot S^\dagger=(S^\dagger_0)^2-2S^\dagger_1 S^\dagger_{-1}\ . \tag{3.4}$$

The allowed isospin is $T=n/2,n/2-2,\ldots,$ 1 or 0, which includes all even-even nuclei.

Although the ground state of the seniority model as given by (3.3) is the product of n zero-coupled pairs, this *does not* mean that nonzero angular momentum pairs cannot be extracted for this state. This seemingly paradoxical statement results from the fact that all nucleons are antisymmetrized with respect to each other. For example, for the four-nucleon system with maximum isospin and projection $T=T_z=2$, the state (3.3) reduces to

$$|\, n=4,T=T_z=2,v=J=0\rangle=[2\Omega(\Omega-1)]^{-1/2}\times S^\dagger_1 S^\dagger_1\,|\,0\rangle\ , \tag{3.5}$$

where $\Omega=j+\frac{1}{2}$ [$\Omega=\sum_j(j+\frac{1}{2})$ for the degenerate many j-shell case] the number of nucleons in the half-filled shell. However, we can recouple the neutron creation operators to get

$$|\, n=4,T=T_z=2,v=J=0\rangle=[2\Omega(\Omega-1)]^{-1/2}\sum_{\substack{JM\\ J\ \text{even}\ M}}(-1)^M A^\dagger_{JM}A^\dagger_{J-M}\,|\,0\rangle\ , \tag{3.6}$$

and $A^\dagger_{JM}$ creates a normalized pair of neutrons coupled to angular momentum J and projection M,

$$A^\dagger_{JM}=\left[\frac{a^\dagger a^\dagger}{\sqrt{2}}\right]^J_M\ , \tag{3.7}$$

where the subscript j has been omitted. Therefore, all angular momenta J and projections M exist with equal probability.

For the many-nucleon system the amplitude for extracting a pair of nucleons with angular momentum J_2 and isospin T_2 from an antisymmetrized n-nucleon state leading to an antisymmetrized $(n-2)$-nucleon state is given by the two-nucleon coefficient of fractional parentage (cfp):

$$\langle j^nT\beta v\alpha J\{\,|\,j^{n-2}T_1\beta_1v_1\alpha_1J_1;j^2T_2v_2J_2\rangle=[(2J+1)(2T+1)n(n-1)/2]^{-1/2}\langle j^nT\beta v\alpha J\|(c^\dagger_{j\tau}c^\dagger_{j\tau})^{J_2T_2}\|j^{n-2}T_1\beta_1v_1J_1\rangle\ , \tag{3.8}$$

where α and β are additional labels needed to specify the many-nucleon states. For the initial state with seniority $v=0$, $v_1=v_2=0$ or 2 and $J_1=J_2$, and α,α_1,β, are unnecessary. For $v_1=0$, then $J_1=0$, $T_1=1$, and β_1 is unnecessary. For $v_1=2$, either J_1 even $\neq0$ and $T_2=1$, or J_1 odd and $T_2=0$, and for J_1 odd β_1 is unnecessary. In the above cfp's β_1 is necessary only for J_1 even $\neq0$ and $T_1=T\pm1$. For $j=\frac{7}{2}$ this occurs only for $n=8$ and $T_1=1$.

The seniority-zero cfp's are given in Table I. In Appendix A we show how to derive these expressions. In general we find that the probability of extracting a pair of nucleons with angular momentum $J>0$ from the seniority zero state is proportional to $2J+1$ which is consistent with (3.6).

The matrix element of any two-nucleon operator can be calculated with the two-nucleon cfp's in terms of the two-nucleon matrix elements of the operator. For matrix elements between seniority-zero states only, the matrix elements of a two-nucleon operator $V^t_{t_z}$, where t is the isospin tensorial rank, become

$$\langle j^nT'T'_zv'=J'=0\,|\,V^t_{t_z}\,|\,j^nTT_zv=J=0\rangle=(-1)^{T+T'+T_z}\begin{pmatrix}T & t & T'\\ T_z & t_z & -T'_z\end{pmatrix}\sum_2 C(nT'T;T_2J_2)(2J_2+1)\langle j^2T_2J_2\|V^t\|j^2T_2J_2\rangle\ , \tag{3.9a}$$

where

$$C(nT'T;T_2J_2)=\frac{n(n-1)}{2}(-1)^{T_2}\frac{[(2T+1)(2T'+1)]^{1/2}}{2J_2+1}\times\sum_1\langle j^nT'v'=J'=0\{\,|\,j^{n-2}T_1;j^2T_2J_2\rangle\langle j^nTv=J=0\{\,|\,j^{n-2}T_1;j^2T_2J_2\rangle\begin{Bmatrix}T' & T & t\\ T_2 & T_2 & T_1\end{Bmatrix}(-1)^{T_1}\ , \tag{3.9b}$$

TABLE I. The two-nucleon cfp's squared and summed over β_1. The quantum number β_1 is necessary only for $T_1 = T \pm 1$ and $J_2 \neq 0$. For $j = \frac{7}{2}$ it occurs in this table only for $n = 8$ and $T_1 = 1$.

T_1	T_2	J_2	$\sum_{\beta_1} \vert \langle j^n T v = J = 0 \{ \vert j^{n-2} \beta_1 T_1; j^2 T_2 J_2 \rangle \vert^2 / (2J_2+1)$
$T+1$	1	0	$\frac{(n-2T)(T+1)(4\Omega+6-n+2T)}{4\Omega n(n-1)(2T+1)}$
$T+1$	1	even >0	$\frac{(n-2T)\{(2\Omega+1)[(2T+3)(n-2T-4)+2]-n-2T-2\}}{8\Omega(\Omega-1)(2\Omega+1)n(n-1)(2T+1)}$
T	0	odd	$\frac{(n-2T)(n+2T+2)}{4\Omega(2\Omega+1)n(n-1)}$
T	1	even >0	$\frac{(n-2T)(n+2T+2)}{4(\Omega-1)(2\Omega+1)n(n-1)}$
$T-1$	1	0	$\frac{(n+2T+2)T(4\Omega+4-n-2T)}{4\Omega n(n-1)(2T+1)}$
$T-1$	1	even >0	$\frac{(n+2T+2)\{(2\Omega+1)[(2T-1)(n+2T-2)-2]+n-2T\}}{8\Omega(\Omega-1)(2\Omega+1)n(n-1)(2T+1)}$

where the double-barred matrix element refers to the isospin space. Since the operator is a scalar, $J_2 = J_2'$, and since in the two-nucleon system the angular momentum determines the isospin, it follows that $T_2' = T_2$, even though the operator may not be an isoscalar. Also for seniority zero cfp's, $v_1 = v_2$ and are determined by $J_1 = J_2$, as mentioned above, and hence v_1, v_2, J_1 are omitted from the notation to save space. Furthermore, from Table I we see that the cfp's for J_2 even $\neq 0$ are equal except for a factor of $\sqrt{2J_2+1}$ and the ones for J_2 odd are equal except for the same factor. Hence the matrix elements of any two-nucleon operator between seniority-zero states in a single j shell depend at most on three two-nucleon matrix elements:

$$\langle V^t \rangle_o = \langle j^2 T = 1, J = 0 \| V^t \| j^2 T = 1, J = 0 \rangle \ , \tag{3.10a}$$

$$\langle V^t \rangle_e = \sum_{J \text{ even} > 0} (2J+1) \frac{\langle j^2 T = 1, J \| V^t \| j^2 T = 1, J \rangle}{(\Omega-1)(2\Omega+1)} \ , \tag{3.10b}$$

$$\langle V^t \rangle_o = \delta_{t,0} \sum_{J \text{ odd}} (2J+1) \frac{\langle j^2 T = 0, J \| V^t \| j^2 T = 0, J \rangle}{\Omega(2\Omega+1)} \ , \tag{3.10c}$$

where $\langle V^t \rangle_{e,o}$ are average matrix elements. Furthermore, we see that for isovector or isotensor operators, the matrix elements depend on only *two* two-nucleon matrix elements since $\langle V^t \rangle_o$ vanishes in these cases.

All the results in this section apply to the seniority model with degenerate single-nucleon energies[15] if we take as Ω,

$$\Omega = \sum_j (j + \tfrac{1}{2}) \ . \tag{3.11}$$

IV. DOUBLE CHARGE EXCHANGE AND THE SENIORITY MODEL

The seniority quantum number is approximately conserved only for nuclei with valence nucleons of the same kind, i.e., nuclei with maximum isospin, $T = n/2$. However, even when it is not quantitatively valid, the seniority model can give qualitative insights.

The double charge exchange operator in (2.1) changes two neutrons into two protons and hence is a two-nucleon isotensor operator, $t = 2$ and $t_z = -2$. The two-nucleon matrix elements of F are

$$\langle j^2 T = 1 J \| F \| j^2 T = 1 J \rangle = 2\sqrt{5} G_J \ , \tag{4.1}$$

where the factor $\sqrt{5}$ is the three-j symbol involved in going to the isospin double-barred matrix element. From (3.10) and the fact that F is an isotensor operator, only two matrix elements will be involved for a transition between seniority-zero states:

$$\langle F \rangle_o = \sqrt{5} \sum_L (-1)^L F_L \ , \tag{4.2a}$$

$$\langle F \rangle_e = \sqrt{5} \left[F_0 - \frac{\Omega+1}{(\Omega-1)(2\Omega+1)} \sum_{\substack{L>0 \\ \text{even}}} F_L - \frac{1}{(2\Omega+1)} \sum_{L \text{ odd}} F_L \right] \ . \tag{4.2b}$$

Hence only the monopole ($L = 0$), the *sum* of the higher even multipoles, and the *sum* of the odd multipoles occur for the DCX between seniority-zero states. The monopole piece has particular physical significance because it corresponds to successive single charge exchanges through the intermediate analog state as seen in (2.6). For the same reason, the monopole part of the DCX operator cannot change the isospin of the target even

TABLE II. The values of X and Y for $j=\frac{7}{2}$, $\Omega=4$.

$n,\bar{n}$	T	Nuclei	$\sqrt{T(2T-1)}$	X	Y	$\sqrt{T(2T-1)}Y$
2	1	^{42}Ca, ^{54}Fe	1	1		
4	2	^{44}Ca, ^{52}Cr	2.4495	0.1111	0.5132	1.2571
6	3	^{46}Ca, ^{50}Ti	3.8730	−0.0667	0.3556	1.3771
6	1	^{46}Ti, ^{50}Cr	1	1.4741		
8	4	^{48}Ca	5.2915	−0.1429	0.2199	1.1638
8	2	^{48}Ti	2.4495	0.1675	0.6184	1.5147

though it is an isotensor operator. This statement is only valid for a single j shell; for many j's there are many monopole operators and only one linear combination is proportional to the isospin generators. With this in mind we define the amplitudes

$$A=F_o-\frac{1}{\Omega}\sum_{L\ \text{odd}}F_L\ , \tag{4.3a}$$

$$B=\sum_{\substack{L>0\\ \text{even}}}F_L-\frac{(\Omega-1)}{\Omega}\sum_{L\ \text{odd}}F_L\ . \tag{4.3b}$$

Hence, if there is no spin dependence, i.e., $F_L=0$, L odd, then the amplitude A is the long-range (monopole) part of the DCX reaction while B is the short-range part. However, spin dependence, while not changing the number of amplitudes that the DCX depends on, will alter the values of the amplitudes. If the spin dependence is dominant, then this separation into long range and short range may no longer be valid. Using Eqs. (3.10), the DCX matrix element for the transition from a target with $T_z=T=(N-Z)/2$, $v=0$, to the double analog state, $T'=T$, $T'_z=T-2$, $v'=0$, is,

$$\langle j^nT,T_z=T-2,v=J=0\,|\,F\,|\,j^nT,T_z=T,v=J=0\rangle=\sqrt{T(2T-1)}\{A+XB\}\ , \tag{4.4a}$$

where

$$X=\frac{1}{(\Omega-1)(2T+3)(2T-1)}\times\left[(n+3)(\Omega+1-n)+\frac{(n-2T)(n+2T+2)(3\Omega+2)}{2(2\Omega+1)}\right]\ . \tag{4.4b}$$

We see from this expression that for a given number of valence nucleons the effect of the monopole amplitude A increases as the isospin increases, but the importance of B with respect to A decreases, i.e., the pairs coupled to isospin zero in (3.3) do not contribute to the monopole part of the DCX. However, for a fixed isospin the contribution of B with respect to A increases as the number of valence nucleons increase.

For targets with identical nucleons only ($T=n/2$) (4.4) reduces to

$$\left\langle j^nT=\frac{n}{2},T_z=\frac{n}{2}-2,v=J=0\,|\,F\,|\,j^nT=T_z=\frac{n}{2},v=J=0\right\rangle=\left[\frac{n(n-1)}{2}\right]^{1/2}\left[A+\frac{(\Omega+1-n)}{(\Omega-1)(n-1)}B\right] \tag{4.5}$$

which agrees with Ref. 10. This formula is valid for the calcium isotopes. If B is zero, then the DCX cross section will increase in proportion to the number of neutron pairs $=T(2T-1)$. However, the fact that B, the short-range part, does not vanish produces the observed cross section[5,6] as discussed in the Introduction.

The DCX transition to the ground state $T'=T-2$ depends on B only because, as we mentioned previously, the monopole term cannot change isospin. This matrix element is given by,

$$\langle j^nT'=T-2,T'_z=T',v'=J'=0\,|\,F\,|\,j^nT,T_z=T,v=J=0\rangle=\sqrt{T(2T-1)}YB\ , \tag{4.6a}$$

where

$$Y=\frac{\Omega}{4(\Omega-1)(2\Omega+1)(2T-1)}\left[\frac{(T-1)(n+2T+2)(n-2T+4)(4\Omega+4-n-2T)(4\Omega+2-n+2T)}{(2T+1)}\right]^{1/2}\ . \tag{4.6b}$$

All of these expressions have a particle-hole symmetry which is consistent with the relation derived in (2.10). This means that the DCX reactions will be the same for particle-hole related nuclei, *except* for the dependence of the pion dynamics on atomic mass, i.e., the mass dependence of the amplitudes A and B.

In Table II the seniority-zero matrix elements are tabulated for $j=\frac{7}{2}$, i.e., $\Omega=4$. We see that the value of X varies substantially for the different isotopes. We also see that for the same target the value of Y is always larger than X indicating that nonanalog transitions are more sensitive to the nonmonopole amplitude than the analog transition.

However for nuclei with $T<n/2$, i.e., nuclei with both protons and neutrons filling the valence shells, seniority will not be a good quantum number. We shall study more realistic transitions for these nuclei in the next section.

V. DCX IN A MORE REALISTIC $(f_{7/2})^n$ MODEL

The seniority quantum number is not conserved for neutrons and protons filling the same major shell,[14] that is, for nuclei with isospin $T < n/2$. We can use more realistic $(f_{7/2})^n$ eigenfunctions to calculate the DCX transition.[14,17–19] The double analog transitions from the calcium isotopes will remain the same since $T = n/2$ in both the initial and final state. However, the transition from the calcium isotopes to the *ground state* of the titanium isotopes will change since these states have lower isospin, $T = n/2 - 2$. Furthermore, the DCX reaction to the double analog with the titanium isotopes as targets will be different from the seniority predictions.

We use a neutron-proton basis for the titanium eigenfunctions.[20] Since the titanium isotopes have two valence protons, the eigenstates have the form

$$\left| j^n T = T_z = \frac{n}{2} - 2, J = 0 \right\rangle = \sum_{vJ} \alpha(n; vJ) \times | (j^2 J; j^{n-2} vJ)^{(0)} \rangle , \tag{5.1}$$

where $\alpha(n; vJ)$ is the amplitude for neutrons with seniority v and angular momentum J.

For the calcium isotopes as targets, the DCX matrix element is derived in Appendix B and given by

$$\left\langle J^n, T = T_z = \frac{n}{2} - 2, J = 0 \mid F \mid j^n, T = \frac{n}{2} = T_z, v = J = 0 \right\rangle = \sum_{L \neq 0} \beta_L(n) F_L , \tag{5.2a}$$

where

$$\beta_L(n) = \frac{1}{2} \left[\frac{n}{\Omega(\Omega-1)} \right]^{1/2} \left[\sqrt{(\Omega-1)(2\Omega+2-n)}\, \alpha(n;00)(-1)^L + 2\Omega\sqrt{n-2} \sum_{J>0} \begin{Bmatrix} j & j & L \\ j & j & J \end{Bmatrix} \sqrt{2J+1}\, \alpha(n;2J) \right] . \tag{5.2b}$$

We note that the neutrons with seniority four do not contribute since the calcium ground states have seniority zero.

Because these transitions are nonanalog the monopole coefficient β_0 equals zero, which also provides a check on the calculation. Hence in general the nonanalog DCX will depend on three complex amplitudes F_L, $L = 2,4,6$, rather than on only one (that is only B) as in the seniority model. We use the wave-function amplitudes α tabulated in Ref. 20 and reproduced in Table III for the titanium isotopes. In Table IV we give the resulting β_L for the calcium isotopes as targets.

From Table III we note that in the titanium isotopes the $J = 0$ and $J = 2$ proton pairs account for more than 95% of the ground-state wave functions. This result is consistent with recent models of nuclear collective motion[21–23] which assume that $J = 0$ and 2 pairs dominate the low-lying states of nuclei. If $\alpha_4 = \alpha_6 = 0$ identically, then $\beta_4 = \beta_6$. Because of this the ratio β_4/β_6 in Table IV is almost the same (~ 0.93–0.97) for all calcium isotopes so that in practice the nonanalog DCX depends on approximately two complex amplitudes for the calcium isotopes.

The DCX matrix element for the double analog transition from the titanium isotopes as targets is derived in Appendix B and given by

$$\left\langle j^n, T = \frac{n}{2} - 2, T_Z = \frac{n}{2} - 4, J = 0 \mid F \mid j^n, T = \frac{n}{2} - 2 = T_Z, J = 0 \right\rangle = \sum \gamma_L(n) F_L , \tag{5.3a}$$

where

$$\gamma_L(n) = -\frac{12(n-2)(n-3)}{\sqrt{2(n-4)(n-5)}} \Omega \sum \alpha(n; \bar{v}\bar{J}) \alpha(n; vJ) \begin{Bmatrix} j & j & L \\ j & j & K \end{Bmatrix} (-1)^{J+\bar{J}} \langle j^{n-2} vJ \{ \mid j^{n-4} v'J'; j^2 K \rangle \langle j^4 v'J' \{ \mid j^2 J; j^2 K \rangle \times \langle j^{n-2} \bar{v}\bar{J} \{ \mid j^{n-4} v'J'; j^2 \bar{K} \rangle \langle j^4 v'J' \{ \mid j^2 \bar{J}; j^2 \bar{K} \rangle , \tag{5.3b}$$

where the cfp's in the above are those for identical particles only and hence the isospin in (3.8) is maximal and the other quantum numbers are not needed. Since the monopole part of the interaction is proportional to the isospin,

$$\gamma_0(n) = \sqrt{T(2T-1)} = \left[\frac{(n-2)(n-3)}{2} \right]^{1/2} .$$

In Table V the $\gamma_L(n)$ are tabulated for ^{46,48}Ti.

The remaining $f_{7/2}^n$ transition to be calculated is the

TABLE III. Values of $\alpha(n; vJ)$ for titanium isotopes. The notation α_{vJ} ($^{40+n}$Ti) is used.

v	J	α_{vJ}(^{44}Ti)	α_{vJ}(^{46}Ti)	α_{vJ}(^{48}Ti)
0	0	0.7608	0.8224	0.9136
2	2	0.6090	0.5420	0.4058
2	4	0.2093	0.0861	0.0196
2	6	0.0812	−0.0127	−0.0146
4	2	0.0	0.0563	0.0
4	4	0.0	−0.1383	0.0

TABLE IV. Values of $\beta_L(n)$ for $^{40+n}\mathrm{Ca}\rightarrow{}^{40+n}\mathrm{Ti}$ (ground state).

L	$\beta_L(n=4)$	$\beta_L(n=6)$	$\beta_L(n=8)$
2	0.7976	0.6574	0.4922
4	1.1284	1.2617	1.1923
6	1.2056	1.3530	1.2343

$^{48}\mathrm{Ti}\rightarrow{}^{48}\mathrm{Cr}$ (ground state). However, the $T=0$ wave functions of ^{48}Cr were not calculated in Ref. 20, and, hence this transition is not calculated in this paper. However, with this exception, all DCX analog and ground-state transitions can be obtained for $f_{7/2}^n$ using the results of Tables IV and V, Eqs. (4.3), (4.5), (5.2), and (5.3), and the particle-hole relations of (2.10).

VI. REACTION-MODEL CALCULATIONS

The purpose of this section is to evaluate the double charge exchange amplitudes F_L [defined in Eqs. (2.3) and (2.4)] within the double-scattering (and meson exchange) models.

A. Sequential single charge exchanges on nucleons

In a full multiple-scattering model the DCX operator F is an explicit function of all of the nucleonic coordinates[11] so it is not a two-nucleon operator as in Eq. (2.1). To apply this equation we must introduce an effective operator which depends explicitly only on the pion coordinates and those of the two neutrons undergoing charge exchange. Implicit dependence on the other nucleonic coordinates may be incorporated through use of distorted pion waves, final-state interactions, etc. A simple and physically reasonable operator of this form arises from the double-scattering model, in which DCX proceeds through two successive single charge exchanges (SCX) (see, for example Refs. 10, 11, and 3).

The DCX operator may be expected to be nonlocal in the nucleon coordinates for two reasons: (1) The pion-nucleon interaction is usually assumed to be nonlocal (typically separable, at least in the P_{33} channel), and (2) the π-nuclear Green's function, which describes the propagation of the π^0 in the nucleus between the two pion-nucleon charge exchanges, is nonlocal. While Eq. (2.2) does not require F to be local in the nucleon coordinates, it is far simpler to calculate and easier to interpret in a local approximation. To this end we make two simplifying assumptions. First, recoil corrections to the pion-nucleon charge exchange operator are approximated by a simple angle transform [see Eq. (6.6)]. Nonlocality still remains in the pion dynamics, but the SCX operator f is now local in the nucleon coordinates. Second, as in Ref. 11, we evaluate the nuclear Hamiltonian in the Green's function at an effective excitation energy. The sum over intermediate nuclear states is evaluated by closure. This renders the DCX operator local in the nucleon coordinates.

TABLE V. Values of $\gamma_L(n)$ for $^{40+n}\mathrm{Ti}\rightarrow{}^{40+n}\mathrm{Cr}$ (double analog).

L	$\gamma_L(n=6)$	$\gamma_L(n=8)$
0	1.0	2.450
2	0.7973	0.2067
4	1.311	0.3790
6	1.269	0.3366

In this section we assume that the pion energy lies below 70 MeV. For these energies the pion-nucleus interaction is relatively weak which allows us to approximate the pion wave function as plane waves at the qualitative level. However, for detailed comparison to data, a proper account of pion distortion is necessary even at these low energies. See Refs. 3 and 24 for the case of ^{14}C and for the relation of the present work to that of Ref. 11. The effect of distortions on Ca isotopes is also treated.

Within the approximations just noted, the DCX operator becomes

$$F(\mathbf{r}_1\mathbf{r}_2,\mathbf{k}',\mathbf{k})=2\left[-\frac{1}{2\pi^2}\right]\int d\mathbf{q}\,\phi_{\mathbf{k}'}^{(-)}(\mathbf{r}_2)^* f(\mathbf{k}',\mathbf{q}) \times\frac{\phi_{\mathbf{q}}^{(+)}(\mathbf{r}_2)\phi_{\mathbf{q}}^{(-)}(\mathbf{r}_1)^*}{k_0^2-q^2+i\epsilon} \times f(\mathbf{q},\mathbf{k})\phi_{\mathbf{k}}^{(+)}(\mathbf{r}_1)\,, \tag{6.1}$$

$f(\mathbf{q},\mathbf{q}')$ is the spin-averaged amplitude for pion-nucleon charge exchange. The right-hand distorted wave $\phi^{(+)}$ represents the incident π^+ wave, the central distorted waves (and accompanying denominator) represent the π^0 propagator, and the left-hand distorted wave represents the outgoing π^- wave. In the DWIA the pion wave functions and propagator are distorted by Coulomb and optical potentials. The overall factor of 2 accounts for the process in which the first charge exchange is on the neutron at position $\mathbf{r}_2$.

The optical potential used for the low-energy distorted waves employed medium corrections (Pauli blocking, nucleon binding energy, Fermi motion, pion annihilation, finite pion-nucleon interaction range, and nucleon recoil) based upon a nonrelativistic model, but with relativistic kinematics. The calculations of DCX at 292 MeV, given in the next section, use free pion-nucleon amplitudes, but do include the effects of pion annihilation and of the finite range of the pion-nucleon interaction.

The multipole components of the double charge exchange amplitude corresponding to this operator are[10] given in (2.3) and are repeated here

$$F_L(\mathbf{k}',\mathbf{k})=G^{Llj}\int d\mathbf{r}_1\,d\mathbf{r}_2 \times\sum_M Y_{LM}(\hat{\mathbf{r}}_1)Y_{LM}^*(\hat{\mathbf{r}}_2)\Psi_{nlj}^2(r_1) \times\Psi_{nlj}^2(r_2)F(\mathbf{r}_1,\mathbf{r}_2,\bar{k}'\bar{k})\,, \tag{6.2}$$

where we have neglected the double-spin flip contribution. These multipole components are used in conjunction with a complete shell-model treatment in Sec. VII. In the seniority model, assuming a spin-independent operator, A is F_0, and B is the sum of the higher multipoles. The radial wave function Ψ_{nlj} is a solution to Schrödinger's equation for a Woods-Saxon potential of

radius $1.3A^{1/3}$ fm and skin thickness 0.5 fm. The well depth is adjusted to reproduce the experimental neutron separation energy for ^{42}Ca. In the simplest calculations we have ignored the variation of the separation energy of the valence neutrons for the different Ca isotopes and for the final double analog state. We will correct for this difference below.

For the plane-wave case the $\mathbf{r}_1$ and $\mathbf{r}_2$ integrations in Eq. (6.2) yield the multipole nuclear form factors

$$H_L(p)=\int r^2\,dr\,j_L(pr)[\Psi_{nlj}(r)]^2 \tag{6.3}$$

in terms of which F_L is

$$-2(2L+1)G^{Llj}\int\frac{d\mathbf{q}}{(2\pi)^3}P_L(\omega)\times\frac{H_L(|\mathbf{k}-\mathbf{q}|)f(\mathbf{k},\mathbf{q})f(\mathbf{q},\mathbf{k}')H_L(|\mathbf{q}-\mathbf{k}'|)}{k_0^2-q^2+i\epsilon}\,, \tag{6.4}$$

where ω is the cosine of the angle between the vectors $\mathbf{k}-\mathbf{q}$ and $\mathbf{q}-\mathbf{k}'$. The three-dimensional integral over the intermediate momentum $\mathbf{q}$ was performed numerically.

We have used a pion-nucleon charge exchange amplitude of the form

$$f(\mathbf{q}',\mathbf{q})=v_0(q')\lambda_0^T(k_c)v_0(q)+v_1(q')\lambda_1^T(k_c)v_1(q)\mathbf{q}'\cdot\mathbf{q}\,. \tag{6.5}$$

If the momenta $\mathbf{q},\mathbf{q}'$ are specified in the π-nucleus center-of-mass frame the λ^T's are given by

$$\lambda_0^T(k_c)=\frac{q}{k_c}\left[\lambda_0(k_c)-\left[\frac{A-1}{A}\right]\left[\frac{q}{k_L}\right]k_c^2\frac{\mu}{m}\lambda_1(k_c)\right]\xrightarrow[A\to\infty]{}\frac{q}{k_c}\left[\lambda_0(k_c)-k_c^2\frac{\mu}{m}\lambda_1(k_c)\right]\,, \tag{6.6a}$$

$$\lambda_1^T(k_c)=\lambda_1(k_c)\,.$$

k_L and k_c are the pion momenta in the laboratory and the π-nucleon center-of-mass frames, and μ is the pion mass, and m is the nucleon mass. The large-A limit was used for the calcium isotopes, in which case we have $q=k_L$. The scattering length λ_0 and volume λ_1 for charge exchange are taken from Ref. 25 for energies below 80 MeV and from Ref. 26 above this energy. Equation (6.6a) also includes, in an approximate fashion, recoil corrections for the struck nucleon. The v's are defined by

$$v_i(q)=\frac{k^2+\alpha_i^2}{q^2+\alpha_i^2},\quad i=0,1\,, \tag{6.6b}$$

where α_i is the range of the pion-nucleon interaction. We have chosen $\alpha_0=1.5$ fm^{-1} and $\alpha_1=1.5$ fm^{-1} to be consistent with previous multiple-scattering calculations.

The absolute values and the relative phase of A and B may be determined directly from the experimental values of the cross sections of the double isobaric analog transition (DIAT) on the calcium isotopes (^{42,44,48}Ca). These were found[6] to be $|A|=0.34$ $(\mu\text{b/sr})^{1/2}$, $|B|=1.45$ $(\mu\text{b/sr})^{1/2}$, $\phi=59°$ at 35 MeV. It is clearly of interest also to determine the cross sections for as many other $f_{7/2}$ isotopes (both analog and ground-state transitions) as is possible to further constrain the strengths of the multipole amplitudes.

The absolute magnitudes of A and B are plotted in Fig. 1. Of note are the following.

(1) The higher multipole contribution B is dominant in the low-energy region 30–60 MeV.

(2) The PWIA and DWIA are qualitatively somewhat similar, but show significant differences. Distortions of the pion wave function are necessary for realistic comparisons with data.

(3) The nuclear medium magnifies A and B in the 30–60 MeV energy range, probably due to the reflection of the π^0 from core since the optical potential is almost real at these energies. At higher and lower energies the distortions are absorptive; the DWIA amplitude is depressed over the PWIA. The effects of pion annihilation and of nuclear excitation become increasingly important at higher energies.

The forward DCX cross sections for ^{42,48}Ca targets are plotted in Fig. 2(a) (PWIA) and 2(b) (DWIA). From Table II the DCX amplitudes for the transitions from the ^{42,48}Ca targets to the DIAS and from the ^{48}Ca target to the ^{48}Ti ground state (GS) are

$$\sqrt{1}(A+B)\ \text{for}\ ^{42}\text{Ca (DIAS and GS transition)}\,, \tag{6.7a}$$

$$\sqrt{6}(A+B/9)\ \text{for}\ ^{44}\text{Ca (DIAS transition)}\,, \tag{6.7b}$$

$$\sqrt{28}(A-B/7)\ \text{for}\ ^{48}\text{Ca (DIAS transition)}\,. \tag{6.7c}$$

The square of the first factor represents the number of

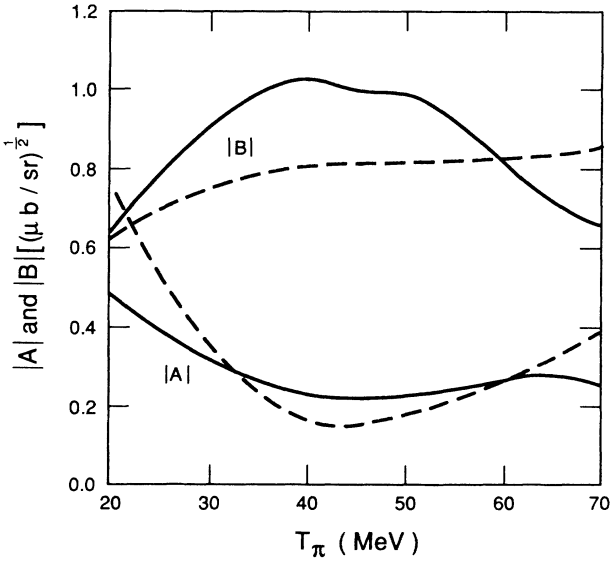

FIG. 1. Absolute value of A and B at 0° for PWIA (dashed) and DWIA (solid) calculations.

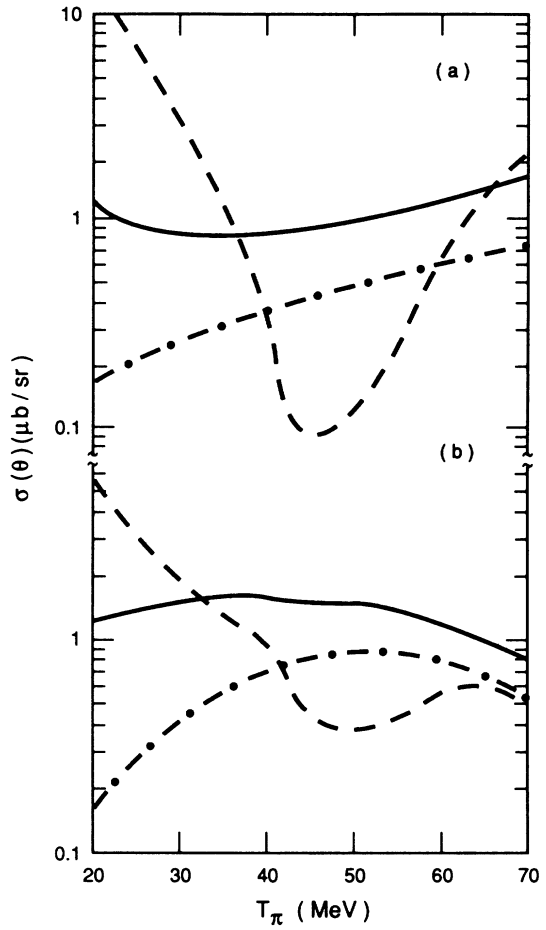

FIG. 2. Forward DCX cross sections for ^{42}Ca (solid) and ^{48}Ca (dashed) transition to the DIAS and the ^{48}Ca→^{48}Ti (g.s.) transition (dash-dot). (a) plane wave; (b) distorted wave.

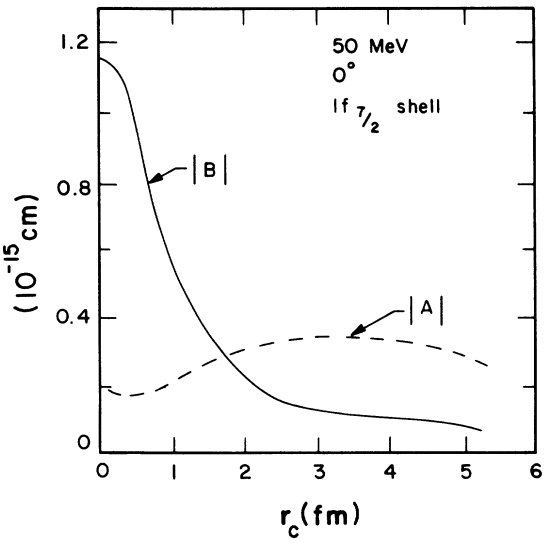

FIG. 3. Absolute values of A and B at 0° and 50 MeV as a function of r_c. The contribution to the PWIA has been omitted for n-n separation less than r_c. The relatively short range of B compared with A is evident.

pairs of valence neutrons. When $|A| \gg |B|$ the cross section for the more neutron-rich isotopes would scale as the pairs factor, but as we have seen $|B|$ is actually several times larger than $|A|$ at low pion energies. The smooth cross section for ^{42}Ca as a function of incident pion energy mirrors $|B|^2$. The numerical factors reduce the role of B in the other isotopes. At 50 MeV, $B/7$ and A tend to cancel producing the decrease in the ^{48}Ca DCX cross section compared to ^{42}Ca, which is consistent with the experimental upper limit of DCX in ^{48}Ca at this energy.[27]

The transition from ^{48}Ca to the ground state of ^{48}Ti is predicted to be larger than that to the DIAS for an incident pion energy in the range 45–55 MeV. The PWIA and DWIA results are qualitatively similar, but the overall magnitude is a strong function of distortions.

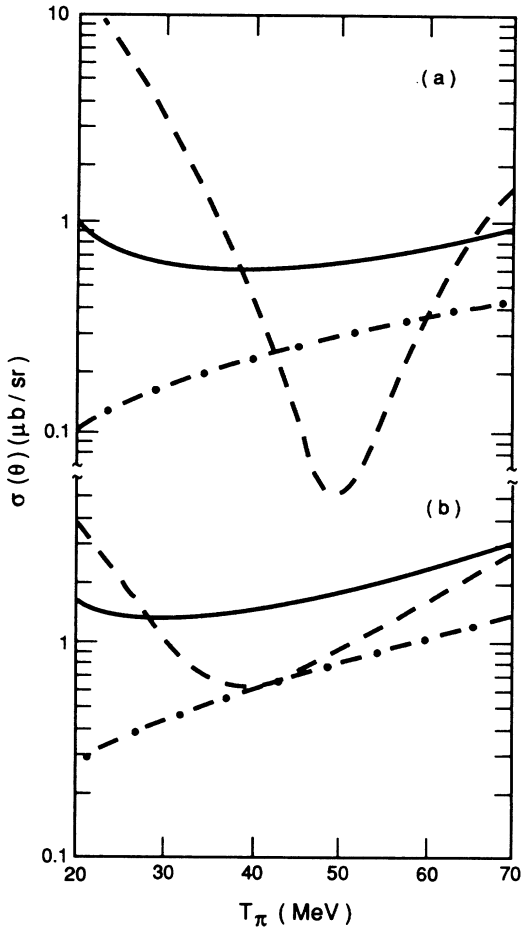

FIG. 4. (a) The effect of hard-core repulsion. Forward DCX cross sections for Ca isotopes [^{42}Ca—solid, ^{48}Ca—dashed, ^{48}Ca→^{48}Ti (g.s.)—dashed-dot] calculated in PWIA. A short-range hard-core repulsion prevents valence neutron pairs from approaching closer than $r_c=0.6$ fm. Compare with Fig. 2, which corresponds to $r_c=0$ fm. Note particularly that the short-range repulsion reduced the DCX cross section of ^{42}Ca and ^{48}Ca (to the ground state of ^{48}Ti). (b) The effect of intermediate range attraction. Forward DCX cross sections for Ca isotopes [see 4(a)] calculated in PWIA. The greater probability of close n-n pairs increased the cross section by roughly a factor of 2. Compare with Fig. 2.

To examine the sensitivity of DCX to the two-neutron separation we have included a step function in the integrand of Eq. (2.3) which vanishes for two-neutron separation of less than r_c, a "hard-sphere" radius. The factor excludes the contribution to DCX from neutron pairs closer than r_c. (The method of calculation is more complicated than presented above and is described in Appendix C.) The results for an incident pion energy of 50 MeV are shown in Fig. 3. The amplitude B falls very rapidly with r_c, which implies that B is determined by the portion of the nuclear wave function for which the "active" neutron pairs are very close ($r<1-2$ fm). Interpreted as a true neutron-neutron hard-sphere repulsion, we conclude that B is sensitive to the short-range portion of the two neutron wave function. In contrast to B, the monopole amplitude A has contributions from n-n separations out to distances comparable to the nuclear radius.

Note that the existence of an additional short-range correlation would also alter the cross section. We use the same formalism as above (Appendix C) to estimate these effects. At this point we go outside the results of the rest of the paper since the introduction of short-range corrections of a Jastrow type is not really done in a manner consistent with shell-model results or at least requires additional assumptions. Figure 4 shows the result of including a repulsive hard core 0.6 fm [Fig. 4(a)] and that of a correlation with intermediate range attraction [Fig. 4(b)]. The point to be made here is that the sensitivity is on the order of a factor of 2.

B. DCX by interaction with the pion cloud

Another possible correction to the results to be presented in the next section is due to the fact that the incident pion may exchange its charge directly with the pion cloud within the nucleus (meson exchange current or MEC). The lowest-order contribution to DCX in plane wave was given in Ref. 28:

$$F(q)=(1/2\pi)\int d^3p/(2\pi)^3\left[\int \Psi^*_{nlj}(\mathbf{r}_1)\sigma_1\cdot\mathbf{p}e^{-i\mathbf{p}\cdot\mathbf{r}_1}v(p)\Psi_{nlj}(\mathbf{r}_1)d\mathbf{r}_1\right]$$
$$\times\frac{1}{p^2+m_\pi^2}g(\mathbf{p}\cdot\mathbf{p}')\frac{2f^2}{m_\pi^2}\frac{1}{p'^2+m_\pi^2}\left[\int \Psi^*_{nlj}(\mathbf{r}_2)\sigma_2\cdot\mathbf{p}'e^{i\mathbf{p}\cdot\mathbf{r}_2}v(p')\Psi_{nlj}(\mathbf{r}_2)d\mathbf{r}_2\right], \quad (6.8)$$

where we have taken

$$g(x)=32\pi(-1.369)\frac{x}{m_\rho^2-m_\pi^2}\left[1-1.423\frac{x}{m_\rho^2-m_\pi^2}\right],$$
$$\mathbf{p}'=\mathbf{p}-\mathbf{q},\quad \mathbf{q}=\mathbf{k}'-\mathbf{k},\quad f^2/4\pi=0.08\ . \quad (6.9)$$

Single-particle states are coupled to give the angular momentum states J,M. $F(q)$ is a function only of the momentum transfer q. The function g derives from a Veneziano-Lovelace representation of the π-π scattering amplitude with a static exchanged pion. We have included form factors $v(p)=\alpha^2/(p^2+\alpha^2)$ for the π-N vertex.

The multipole projections of this operator are, for the nlj shell,

$$F_L=\frac{6(2L+1)}{\pi^2}\left[\frac{f^2}{4\pi}\right]\int\frac{d^3p}{(2\pi)^3}H_L(p)H_L(p')$$
$$\times g(\mathbf{p}\cdot\mathbf{p}')P_L(\hat{\mathbf{p}}\cdot\hat{\mathbf{p}}')\ , \quad (6.10a)$$

where

$$H_L(p)\equiv\sum_\lambda D_{\lambda Llj}pH_\lambda(p)\frac{v(p)}{p^2+m_\pi^2}$$
$$\times\sqrt{(2\lambda+1)}\begin{bmatrix}\lambda & 1 & L\\ 0 & 0 & 0\end{bmatrix}(-1)^{\lambda/2}\ , \quad (6.10b)$$

and $H_\lambda(p)$ is defined by Eq. (6.3), and $D_{\lambda Llj}$ is defined in (2.4b). The azimuthal integral is trivial; the two remaining integrals were performed numerically. [The substitution $\mathbf{s}\equiv\mathbf{p}-\mathbf{q}/2$, which implies $\mathbf{p}=\mathbf{s}+\mathbf{q}/2$, $\mathbf{p}'=\mathbf{s}-\mathbf{q}/2$ and $\mathbf{p}\cdot\mathbf{p}'=\mathbf{s}^2-(\mathbf{q}/2)^2$, is convenient.] From (2.4a) we see that amplitudes with L odd only contribute to the spin-dependent part of the pion-nucleon interaction.

shell with $T=n/2$ and amplitudes with L odd only is given by (4.3) and (4.5) and reduces to:

$$\frac{d\sigma}{d\Omega}=\frac{n}{2(n-1)}\left|\sum_{\substack{L\\ \text{odd}}}F_L\right|^2. \quad (6.11)$$

The term proportional to the "pairs factor," $n(n-1)/2$, is not present. For the isotopes ^{42}Ca, ^{44}Ca, ^{46}Ca, ^{48}Ca the coefficients in Eq. (6.11) are 1, 0.666, 0.600, 0.571.

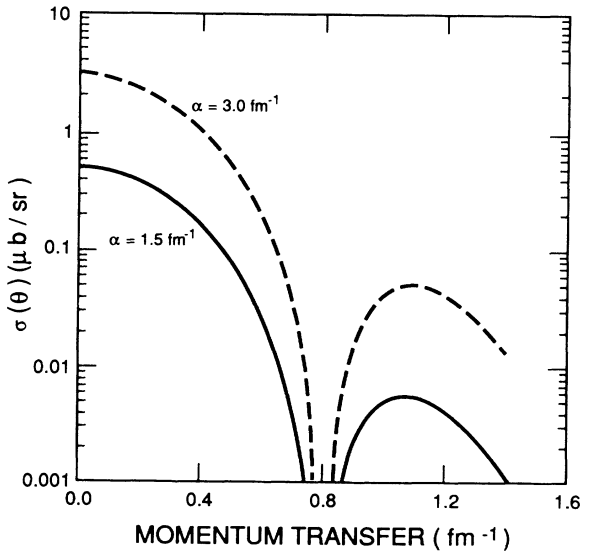

FIG. 5. Meson exchange current contribution to DCX at ^{42}Ca. Cross sections for the other isotopes may be obtained by scaling from Eq. (C9). The two-step process is assumed negligible for this figure.

The strong sensitivity of the MEC contribution to DCX on ^{42}Ca as a function of the range α of the vertex function is shown in Fig. 5 for two values of α. The contribution is comparable to the sequential process for intermediate values of the range (3.0 fm^{-1}), which corresponds to an rms nucleon radius of 0.8 fm. In principle one should add this (real for the case of plane waves) amplitude to that of the sequential process. However, the two contributions are not computed within a single unified theory, and so it is possible that there might be some double counting, especially if the nucleons are very close. The effect of pion distortions on the MEC amplitude is presently under study.

VII. DCX CROSS SECTIONS

Since the DCX operator (2.1) is a two-nucleon operator, once the DCX reaction is known for two nucleons coupled to angular momentum $J=0,2,\ldots,2j-1$ in a shell-model orbit j, then it can be determined for many nucleons in that orbit. For the seniority-model Eqs. (4.3), (4.4), and (4.6) determine the dependence on the many-valence nucleons. For a more realistic model, (5.2) and (5.3) plus Tables IV and V determine this dependence. In order to get an estimate of the difference between the two models, we have used the DCX scattering model of the last section. In this model the DCX proceeds through two successive pion single charge exchanges with closure over the intermediate nuclear states and with pion distortions taken into account. The F_L have been calculated in this model and the nuclear-structure results of the preceding sections have been used to calculate the differential cross sections. We have included neither the effect of a short-range repulsion nor charge exchange from the pion cloud in the following comparisons with data. The final excitation energy E^* was taken as the value appropriate for a given nucleus and the "closure" energy was taken as zero; i.e., the intermediate π^0 has the same energy as the initial π^+.

The measured cross section[29,30] at pion energy of 292

TABLE VI. DCX cross sections at $\theta=5°$ and $T_\pi=292$ MeV. When two numbers are given in brackets the upper value is for the seniority model and the lower is with the wave functions of Ref. 20. For the other cases the two results are the same. For ^{48}Ti the seniority model is not the same as the full model but no values are given in Ref. 20 for the ^{48}Cr ground-state wave function. The theoretical values were calculated with distorted waves. The data and fit were taken from Refs. 29 and 30. The fits were only to the analog values with no variation in distortion across the shell assumed.

Transition	$\frac{d\sigma}{d\Omega_{\rm exp}}$ ($\theta=5°$) (μb/sr)	$\frac{d\sigma}{d\Omega_{\rm fit}}$ ($\theta=5°$) (μb/sr)	$\frac{d\sigma}{d\Omega_{\rm th}}$ ($\theta=5°$) (μb/sr)
Analog transitions			
^{42}Ca→^{42}Ti	0.404±0.061	0.404	0.352
^{44}Ca→^{44}Ti	0.600±0.096	0.562	0.784
^{46}Ca→^{46}Ti			1.345
^{46}Ti→^{46}Cr			[0.350 0.224]
^{48}Ca→^{48}Ti	1.746±0.290	1.714	1.925
^{48}Ti→^{48}Cr	0.590±0.103		[0.586 0.540]
^{50}Ti→^{50}Cr	0.968±0.201	1.025	0.947
^{52}Cr→^{52}Fe	0.574±0.111	0.562	0.388
^{54}Fe→^{54}Ni			0.127
Ground-state transitions			
^{44}Ca→^{44}Ti	0.014±0.014	0.306	[0.077 0.036]
^{46}Ca→^{46}Ti			[0.079 0.025]
^{48}Ca→^{48}Ti	≤0.045	0.262	[0.049 0.014]
^{48}Ti→^{48}Cr			[0.081]
^{50}Ti→^{50}Cr	≤0.066	0.367	[0.057 0.018]
^{52}Cr→^{52}Fe	≤0.028	0.306	[0.041 0.019]

MeV and scattering angle $\theta=5°$ are reproduced in column two of Table VI. In the third column is a fit[29] to the seniority model treating A and B as parameters in the DIAS formula given in Eq. (4.5). In the last column are the calculated results in both the seniority model and the more realistic model. For the DIAS transition the two models are the same for these isotopes which all have $T=n/2$ or $T=\bar{n}/2$, where $\bar{n}$ is the number of holes. For transitions to the ground states, which do not have maximal isospin, the seniority-model result is given on the top, the more realistic model on the bottom. For the ^{48}Ti→^{48}Cr (ground-state) transition the realistic calculation has not been done yet, as discussed in Sec. V.

The seniority-model fit to the DIAS (third column) predicts too large a cross section to the non-DIAS ground-state transition, which is consistent with the fact that seniority is not a good quantum number.

On the other hand, the calculated results show good agreement with the double analog transitions (DIAS). In particular the experimental cross sections do not increase as the number of pairs $n(n-1)/2$, as indicated in the Introduction, and the calculated cross sections reproduce

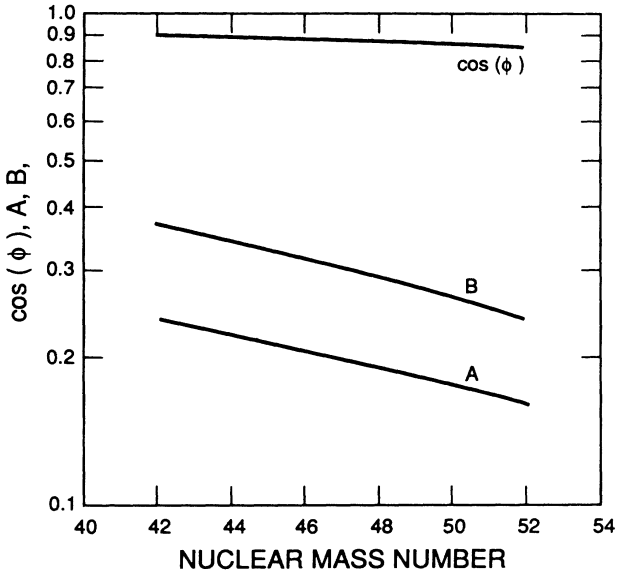

FIG. 6. Variation of $|A|$, $|B|$, and cosϕ with the nuclear mass number at 292 MeV.

TABLE VII. DCX cross sections at low energy. The data are from Refs. 6 and 27.

			$\theta=5°$	
	$T_\pi=35$ MeV	$\theta=40°$	$T_\pi=35$ MeV	$T_\pi=45$ MeV
	$\frac{d\sigma}{d\Omega_{\text{exp}}}$	$\frac{d\sigma}{d\Omega_{\text{th}}}$	$\frac{d\sigma}{d\Omega_{\text{th}}}$	$\frac{d\sigma}{d\Omega_{\text{th}}}$
Transition	(μb/sr)	(μb/sr)	(μb/sr)	(μb/sr)
Analog transitions				
^{42}Ca→^{42}Ti	2.0±0.5	0.719	1.534	1.485
^{44}Ca→^{44}Ti	1.1±0.3	0.545	0.867	0.740
^{46}Ca→^{46}Ti		0.526	0.607	0.409
^{46}Ti→^{46}Cr		1.394 0.705	3.801 1.591	2.902 1.667
^{48}Ca→^{48}Ti	2.4±0.7	1.464	1.321	0.443
^{48}Ti→^{48}Cr		1.053 0.914	1.645 1.290	1.081 0.858
^{50}Ti→^{50}Cr		1.164	1.279	0.611
^{52}Cr→^{52}Fe		0.768	1.239	0.700
^{54}Fe→^{54}Ni		0.833	1.894	1.449
Ground-state transitions				
^{44}Ca→^{44}Ti		0.659 0.338	1.610 0.873	1.583 0.954
^{46}Ca→^{46}Ti		0.791 0.299	1.932 0.810	1.890 0.972
^{48}Ca→^{48}Ti		0.608 0.221	1.373 0.552	1.414 0.761
^{48}Ti→^{48}Cr		1.030	2.269	2.395
^{50}Ti→^{50}Cr		0.472 0.315	1.875 0.762	1.980 0.981
^{52}Cr→^{52}Fe		0.624 0.324	1.719 0.943	1.490 0.954

the trend with atomic mass. The transitions to the ground state have large experimental errors, in fact the measured cross sections are primarily upper limits. For two targets, ^{44}Ca and ^{52}Cr, which are particle-hole conjugates of each other, the seniority results are larger than the upper limits, while for the remaining ground-state transitions the seniority results are within the upper bounds. However, the realistic wave-function results are all within the upper limits. The change in the cross sections with the realistic wave functions is quite large, in all cases the cross sections are reduced by a factor of 2–4 from the seniority model. In Fig. 6 the calculated values of A and B are given as a function of mass number. These amplitudes follow an $A^{-10/3}$ behavior similar to that predicted in an eikonal model.[31]

In Table VII the measured cross sections[6,27] (column two) for a lower energy, $T_\pi = 35$ MeV, but a larger angle, $\theta = 40°$, are compared to the calculated cross sections in both the seniority and the realistic $(f_{7/2})^n$ model. At the lower energy the DIAS cross sections are larger than at $T_\pi = 292$ MeV, and the trend with atomic mass is different. The calculated values are about a factor of 2 smaller than the measured values, but are much better than the results taking the monopole alone.

However, as noted in the Introduction, the experimental cross sections do not increase with atomic mass, and this trend is given correctly by the calculated cross sections. This mass dependence reflects the importance of the short-range correlations at this pion energy, i.e., the importance of B in (4.5). The fact that the calculated values at this energy do not agree as well indicates that other configurations may play a role, other sources of correlations may also be involved, or the MEC contribution should be included (Sec. VI).

The differential cross section for the DIAS on ^{48}Ca is shown in Fig. 7. Distortion of the pion wave function has the effect of raising the large-angle and lowering the forward-angle cross section. The kinematical effect of the excitation energy E^* of the residual nucleus ^{48}Ti is included in the calculation of the pion-nucleon amplitudes and in the energy used in calculating the pion wave functions. The net effect is to increase the differential cross section without greatly changing its shape.

The angular dependence of DCX on the different isotopes of Ca is very different as may be seen from Fig. 8. These sharp differences are due to the different contributions of the short-range part B to the DCX cross sections as seen in (6.7). The inversion of the double analog transitions in ^{42}Ca and ^{48}Ca noted in Fig. 2 is seen to occur only for smaller angles in this model. The measured angular distribution[27] of ^{48}Ca shows a flat angular distribution similar to the calculated DCX angular distribution, although the calculated values disagree in magnitude. Measurement of the angular distributions of the other isotopes will determine the role of short-range correlations.

The calculations also indicate that the ground-state transitions will be comparable to the DIAS rather than an order of magnitude smaller as at $T_\pi = 292$ MeV. We see in Table VII that this is particularly true at the smaller angles (column four) and at $T_\pi = 45$ MeV (column five) for which the ground-state transition is predicted to be larger than the DIAS. This means that the DCX can probe the change of the ground states of nuclei as a pair of neutrons are converted into a pair of protons. Recent models of nuclear collective motion[21–23] suggest that low-lying collective states of nuclei are composed primarily of coherent pairs of neutrons and protons coupled

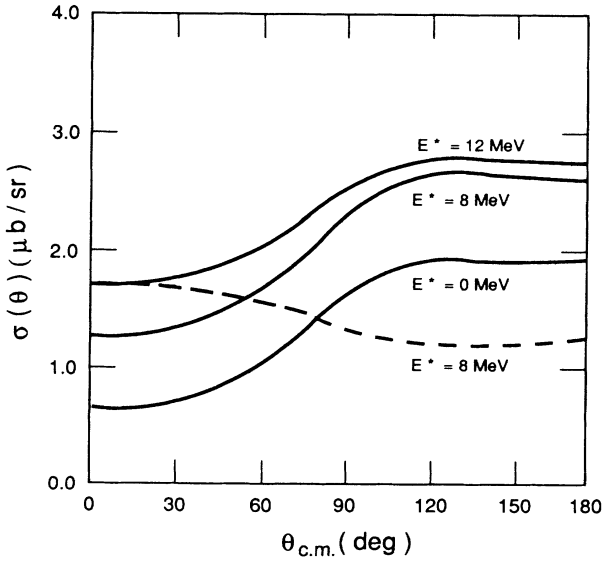

FIG. 7. Angular distribution of DCX on ^{48}Ca at 35 MeV. The solid curves are calculated with distorted wave, and the dashed curve is a plane-wave calculation. The distortions raise the cross section at the back angles. The kinematic effect of the excitation energy E^* of the final product nucleus is shown for three cases.

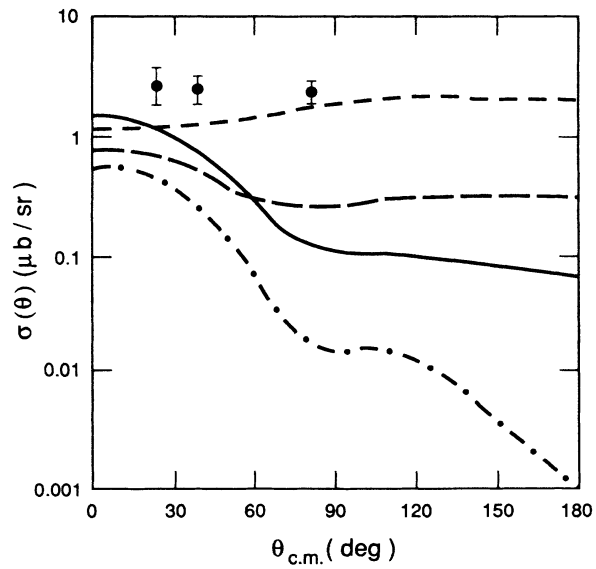

FIG. 8. Angular distribution of several calcium isotopes at 35 MeV. The analog transitions are ^{42}Ca (solid), ^{48}Ca (dashed), and ^{44}Ca (long dash) and the ground-state transition in ^{48}Ca is the dash-dot curve. The data (Ref. 27) are for ^{48}Ca. Despite the influence of the "pairs" factor the ^{42}Ca cross section is larger at small angles than that of other Ca isotopes.

to angular momentum $J^\pi=0^+,2^+$. This DCX reaction could test these models.

VIII. SINGLE CHARGE EXCHANGE

In certain cases the seniority scheme could be of use in providing relations among cross sections of a single charge exchange reaction. For a (π^+,π^0) transition in a j^n configuration we must distinguish among several situations. We will first discuss an analog transition, i.e., a transition in which the final state is the isobaric analog of the ground state of the target.

A. Analog transition; n-even seniority $v=0$

Let us consider states with maximum isospin in the j^n configuration. In this case the initial and final states of the nucleus have $J=0^+$ and the only transition operator $f^{(k)}$ that will contribute is a scalar in the spatial and spin coordinates (i.e., $k=0$) and therefore only the monopole term will enter the calculation. In this case the amplitude for the transition will involve the matrix element

$$\left\langle j^n,v=0,J=0\left|\sum_i f^{(0)}(i)\right|j^n,v=0,J=0\right\rangle = n\langle j\,|\,f^{(0)}\,|\,j\rangle\ . \quad (8.1)$$

The cross section is obtained by taking the square of this matrix element and dividing it by the normalization squared for the isobaric analog state (IAS), i.e., by n. Thus

$$\sigma=\frac{n}{2}\sigma(j^2,v=0) \quad (8.2)$$

where $\sigma(j^2,v=0)$ is the single charge exchange cross section for the case of $T=1$. This is, of course, a familiar result, telling as that for even-even nuclei the single charge exchange reaction is proportional to $(N-Z)$.

B. Analog transition; n-odd seniority $v=1$

The case of $j^n(v=1,J=j)$ is more complicated and so far not fully explored experimentally. The matrix element contributing to the cross sections can be written in general, in terms of irreducible tensors[7] of rank k as

$$A^{(k)}(j^n,v=1,J=j) = \left\langle j^n,v=1,J=j\left|\sum_i f^{(k)}(i)\right|j^n,v=1,J=j\right\rangle\ . \quad (8.3)$$

Note that now not only $k=0$ may contribute but in principle all k that satisfy $|\mathbf{j}+\mathbf{k}|=|\mathbf{j}|$. Following seniority relationships[7] one can write simple expressions for this matrix element if one distinguishes between the cases $k=0$, k odd and $k>0$ even.

For the monopole case ($k=0$) one has the simple relation

$$A^{(0)}(j^n,v=1,J=1)=n\langle j\,|\,f^{(0)}\,|\,j\rangle\ , \quad (8.4)$$

where $\langle j\,|\,f^{(k)}\,|\,j\rangle$ denotes a matrix element for $n=1$ (in this case $k=0$). For $k>0$ and even one finds[7] the expression:

$$A^{(k)}(j^n,v=1,J=j)=\frac{\Omega-n}{\Omega-1}\langle j\,|\,f^{(k)}\,|\,j\rangle\ . \quad (8.5)$$

Finally for k odd one obtains

$$A^{(k)}(j^n,v=1,J=j)=\langle j\,|\,f^{(k)}\,|\,j\rangle\ . \quad (8.6)$$

In principle for any angle and any energy of the incoming pion the charge exchange scattering amplitude will contain all three kinds of amplitudes with a number of different k contributing. After taking into account again the normalization of the IAS one can write

$$\sigma(j^n,v=1,J=j)=\frac{1}{n}\left|n\alpha+\frac{\Omega-n}{\Omega-1}\beta+\gamma\right|^2\ , \quad (8.7)$$

where the coefficients α, β, and γ are complex and are functions of scattering angle and incident energy of the pion. Their values, of course, depend on the particular properties of the wave functions of the bound nucleon in the j orbit. The coefficients α, β, and γ, however, are independent of n. Therefore, one can relate the cross sections for various isotopes (or isotones) for nuclei which are well described by a single configuration j^n. Applying this formula to the ground-state analog transitions in the odd-n Ca isotopes one gets the formulas for the cross sections as shown in Table VIII.

The coefficients in these expressions are complex and therefore we deal *a priori* with a five-parameter problem (three absolute values and two relative phases), and the data for the odd-n Ca isotopes will not be sufficient to check this relation. One should, however, note that for a certain choice of angles and energies one can minimize the contributions of one of the parameters. For example, the parameter γ is due to the contribution of odd-rank spherical tensors and it involves the spin degree of freedom of the nucleon. By choosing a forward-scattering angle one may possibly neglect this term. For pion energies around the (3,3) resonance the spin-dependent (π^+,π^0) transition is more than an order of magnitude smaller than the spin-independent one.[32,33]

In the past only very few charge exchange reactions on an odd-even nucleus were studied. The case of ^{7}Li was considered and the $L=2$ in addition to the $L=0$ transfer was calculated.[32,33] The case of ^{13}C(gs)$\rightarrow$ ^{13}N(gs) requires only $L=0$ ($k=0$ and $k=1$) transfer and was studied extensively in the past.[32] Of course the application of Eq. (8.7) is probably limited because there are not many series of nuclei in which the ground states can be described as $j^n(v=1)$ configurations.

TABLE VIII. Single charge exchange cross sections for odd calcium isotopes.

Nucleus	Cross section
^{41}Ca	$(\alpha+\beta+\gamma)^2$
^{43}Ca	$\frac{1}{3}(3\alpha+\frac{1}{3}\beta+\gamma)^2$
^{45}Ca	$\frac{1}{5}(5\alpha-\frac{1}{3}\beta+\gamma)^2$
^{47}Ca	$\frac{1}{7}(7\alpha-\beta+\gamma)^2$

C. Nonanalog transition in the j^n configuration

It is clear from the study of pion double charge exchange that transitions to nonanalog states are very important intermediate steps in the excitation of double isobaric analog resonances (especially for low-pion energies). It is, therefore, of considerable interest to study single charge exchange to nonanalog states.

We will now write relations among charge exchange cross sections for nonanalog transitions between the ground states of a j^n configuration (with isospin $T=T_{\max}$) and states of the same j^n configuration but differing in total spin and seniority (but not total isospin).

For an amplitude of a transition between a state with seniority $v-2$ to a state with seniority v and maximum isospin the relevant matrix element can be expressed[7] as

$$\left\langle j^n v J' \left| \sum_{i=1}^{n} f^{(k)}(i) \right| j^n v-2J \right\rangle = \left[\frac{(n-v+2)(2\Omega+2-n-v)}{2(2\Omega+2-2v)} \right]^{1/2} \left\langle j^v v J' \left| \sum_{i=1}^{v} f^{(k)}(i) \right| j^v v-2J \right\rangle , \tag{8.8}$$

where k even >0. The meaning of the expression is that the one-body matrix element of n particles in a j orbit and defined seniority can be expressed in terms of a matrix element of v particles in the orbit j. This is usually referred to as the reduction formula. The corresponding cross section can be written as

$$\sigma(j^n v-2J \to j^n v J') = \frac{(n-v+2)(2\Omega+2-n-v)v}{2(2\Omega+2-2v)n} \times \sigma(j^v v-2J \to j^v v J') . \tag{8.9}$$

The extra factor v/n that appears here results from the fact that when we normalize the analog states in the n-body system we need a factor $1/\sqrt{n}$ and in the v-body system a factor $1/\sqrt{v}$.

For the case of $v=2$ (n even) we obtain

$$\sigma(j^n 0J \to j^n 2J') = \frac{(2\Omega-n)}{2(\Omega-1)} \sigma(j^2 0J \to j^2 2J') \tag{8.10}$$

and for n odd $v=3$ we obtain

$$\sigma(j^n 1J \to j^n 3J') = \frac{3}{4}\frac{n-1}{n}\frac{(2\Omega-1-n)}{(\Omega-2)} \times \sigma(j^3 1J \to j^3 3J') . \tag{8.11}$$

We can, therefore, for a given J and J' relate a transition in the j^n system to the j^2 (or j^3) system. For example, in the calcium isotopes one obtains (for given $J \to J'$ transitions) the following relations:

$$\begin{aligned} \sigma(^{44}\mathrm{Ca} \to {}^{44}\mathrm{Sc}) &= \tfrac{2}{3}\sigma(^{42}\mathrm{Ca} \to {}^{42}\mathrm{Sc}) , \\ \sigma(^{46}\mathrm{Ca} \to {}^{46}\mathrm{Sc}) &= \tfrac{1}{3}\sigma(^{42}\mathrm{Ca} \to {}^{42}\mathrm{Sc}) , \\ \sigma(^{45}\mathrm{Ca} \to {}^{45}\mathrm{Sc}) &= \tfrac{3}{5}\sigma(^{43}\mathrm{Ca} \to {}^{43}\mathrm{Sc}) . \end{aligned} \tag{8.12}$$

IX. THE SINGLE AND DOUBLE CHARGE EXCHANGE REACTIONS IN THE GENERALIZED SENIORITY SCHEME

Very often in nuclei the various j_α orbits are nondegenerate, and one is faced with the problem of configuration mixing involving several shell-model nondegenerate orbits. The introduction of a seniority quantum number in this case is more complicated,[16,34,35] and its validity is not always clear. However, in some cases the introduction of the generalized seniority scheme may be of use.

The way one proceeds is to generalize the operators in Eq. (2.1) by introducing[16]

$$S_q^\dagger = \sum C_j S_q^\dagger(j) \tag{9.1}$$

where now $C_j \neq 1$. These $S_q^\dagger$ operators are then used to generate generalized seniority $\tilde{v}$ states. A state of an even-even nucleus with n identical nucleons of seniority $\tilde{v}$ outside the closed shells is given in this scheme by

$$|\, \tilde{j}^{\,n} \tilde{v} J \rangle = \eta^{-1} (S_1^\dagger)^{(n-\tilde{v})/2} |\, j^{\tilde{v}} \tilde{v} J \rangle , \tag{9.2}$$

where $\tilde{j}$ denotes symbolically a generalized orbit given by $\tilde{j}=\Omega-\frac{1}{2}$, $\Omega=\sum_{j_\alpha}(j_\alpha+\frac{1}{2})$ is half the size of the single-nucleon space, and η^{-1} is a normalization constant. In particular a $\tilde{v}=0$, $J=0$ state is obtained by

$$|\, \tilde{j}^{\,n}, \tilde{v}=0, J=0 \rangle = \eta^{-1} (S_1^\dagger)^{n/2} |\, 0 \rangle , \tag{9.3}$$

where $|\,0\rangle$ is the ground state of the closed shell nucleus.

The above scheme of generalized seniority with the operators given in Eq. (9.1) does not have the simple algebraic properties that the operators (3.1) have and of course much of the simplicity is lost. Under certain approximations relations among matrix elements that are valid in the degenerate j case remain true also in the generalized seniority scheme.[16,36,37] In particular a reduction formula analogous to the one in Eq. (4.5) is valid if the two-nucleon operator has similar properties as the effective interaction. In that case, the two-nucleon operator can be written as a sum of two terms, one that is linear in n and the second term quadratic. Thus

$$\langle \tilde{j}^{\,n}, \tilde{v}=0, J=0 \,|\, F \,|\, \tilde{j}^{\,n}, \tilde{v}=0, J=0 \rangle = \frac{n(n-1)}{2}\alpha + \frac{n}{2}\beta . \tag{9.4}$$

The generalized seniority scheme, when valid, describes only even-even nuclei in which the active nucleons are of the same kind, i.e., either neutrons only or protons only. In our application of this scheme to the charge exchange reactions we will refer to such kinds of nuclei only.

A. The single charge exchange reaction in the generalized seniority case

The relations in Sec. VIII apply also for the case of many degenerate orbits (i.e., the quasispin limit of the generalized seniority $C_{j_\alpha}=1$). The case of nondegenerate j_α orbits is more complicated and there is no such a simple reduction formula as above.

B. The double charge exchange reaction

The application of the generalized seniority scheme to double charge exchange is richer in its content and more interesting than its application to the single charge exchange discussed above.

First of all Eq. (4.5) holds in the degenerate case and to a *good approximation* also in the nondegenerate generalized seniority case if the DCX operator has similar properties as the effective interaction operator:

$$\sigma_{\mathrm{DCX}}(\tilde{j}^{\,n},\tilde{v}=0,J=0) = \frac{n(n-1)}{2}\left[\tilde{A}+\frac{(\Omega+1-n)}{(\Omega-1)}\frac{\tilde{B}}{(n-1)}\right]^2 . \quad (9.5)$$

The coefficients $\tilde{A}$ and $\tilde{B}$ cannot be related in a simple way to the kinds of coefficients A and B as in the case of a pure j^n configuration. Again, however, as in the pure j^n configuration case, the DCX cross section is given in terms of three parameters, the two absolute values of $\tilde{A}$ and $\tilde{B}$ and the relative phase between the two. One can, therefore, write Eq. (9.5) for $n=2,4,6$ and express the higher n ($n=8,10\ldots$, etc.) cross sections in terms of the cross sections for $n=2,4,6$. For example, one can derive for $n=8$ the relation:

$$\sigma_8=\frac{4\sigma_2-12\sigma_4+20\sigma_6}{7} , \quad (9.6)$$

where we used the notation $\sigma(\tilde{j}^{\,n},\tilde{v}=0,J=0)\equiv\sigma_n$.

C. The Ni isotopes; an application of a generalized seniority scheme

Among the many nuclei studied, the Ni isotopes are probably the best example of the use of the generalized seniority scheme. In several theoretical papers[16,34,35] it was pointed out that one can successfully describe the spectra, of these isotopes in terms of some kind of generalized definition of seniority. In the early papers[15] the degenerate orbit quasispin formalism was introduced for the purpose of studying the energy levels of these isotopes. The $p_{3/2}$, $p_{1/2}$, and $f_{5/2}$ orbits of the active shell-model space are, however, not really degenerate, and the use of a generalized seniority scheme which takes into account this fact is necessary. In an exact shell-model calculation[35] which included all configurations made of $j_\alpha=p_{3/2}$, $p_{1/2}$, and $f_{5/2}$ orbits, it was demonstrated that the ground states and the first excited $J=2^+$ states in the even Ni isotopes are extremely well described by the $\tilde{v}=0$ and $\tilde{v}=2$ states[16] given by Eq. (9.2).

The coefficients $C_{3/2}$, $C_{1/2}$, and $C_{5/2}$ of the S_+ operator are defined by the ^{58}Ni ground-state wave function and the $|\,\tilde{j}^{\,2},\tilde{v}=2,J=2^+\rangle$ basic state by the first excited $J=2^+$ in ^{58}Ni. The ground-state energies of the even-Ni isotopes are very well described[16,34,35] by the formula in Eq. (9.4).

Both the experimental and theoretical results[35] for the (p,t) cross section show a behavior, as a function n, characteristic of a generalized seniority $\tilde{j}^{\,n}$ configuration. The (p,t) cross sections for gs to gs transitions should, in the case of a single j peak, in the middle of the shell, i.e., $n=\Omega$. In fact in the Ni isotopes the maximum in these (p,t) cross sections occurs for ^{62}Ni, i.e., $n=\Omega$. It is, therefore, reasonable to apply the formalism of single and double charge exchange reactions developed in previous subsections to the Ni isotopes.

The even isotopes of Ni are stable targets, and the experimental and theoretical implications could be verified in (π^+,π^-) experiments. One could measure, for example, the nonanalog single charge exchange transitions between the $J=0^+$ ground states and the analog of the first excited $J=2^+$ states which are 1.3–1.5 MeV above the ground states in the various Ni isotopes. A decreasing linear n dependence is expected in accordance with Eq. (8.10). As for the double charge exchange reaction, it is of interest to test Eq. (9.5) or equivalently the relation Eq. (9.6) among the DIAS cross sections for ^{58}Ni, ^{60}Ni, ^{62}Ni, and ^{64}Ni.

Such experiments we believe will not only tell us more above the reaction mechanism but also open new possibilities of studying nuclear structure with the particular emphasis on the nuclear correlations.

X. SUMMARY AND CONCLUSIONS

In this paper we have calculated the lowest-order pion double charge reaction mechanism using shell-model wave functions of medium weight nuclei. We have used the sequential reaction mechanism in which the pion undergoes two single charge exchange scatterings on the valence neutrons. The distortions of the incoming, intermediate, and outgoing pion are included. The closure approximation is made for the intermediate states with an average excitation energy used in the pion propagator. The double charge exchange is assumed to take place on the valence nucleons which are assumed to be in one spherical shell-model orbital.

The distortion of the intermediate π^0 is important. At low energies (30–60 MeV) this distortion enhances the DCX cross section over the plane-wave approximation for the π^0 propagation. This enhancement is probably due to reflection from the core, since the optical potential is almost real.[38]

Within certain assumptions it is shown that in the seniority model the DCX for all the isotopes is given in terms of two complex amplitudes. One amplitude is primarily sensitive to the short-range correlation of the valence nucleons and spin dependence of the DCX amplitude; the other amplitude to the long-range behavior as seen from Fig. 3. Furthermore, the relative importance of these two amplitudes depends very much on the pion energy (Fig. 1). In particular at pion energies between 30–60 MeV the DCX seems to be dominated by the be-

havior of the nucleons about 1–2 fm apart. Experimentally this feature is demonstrated for pion DCX on the calcium isotopes[5,6,27,29,30] by the observation that these cross sections do not increase by the number of valence neutron pairs. The angular distributions will also be sensitive to the short-range correlations. The calculations in this paper are able to reproduce the observed cross sections and their trend with atomic mass for the higher pion energy (292 MeV) as seen in Table VI. For the lower pion energies the trend with atomic mass and angular distribution are reproduced but the magnitudes are underestimated (Table VII and Fig. 8). These results suggest that the spin dependence of the pion-nucleon scattering amplitude or additional correlations due to configuration admixing or extra-nuclear effects such as the pion cloud (Fig. 5) or quarks[39] may be important.

For pion energies for which the short-range correlations are important, the excitation of the ground state is comparable to the DIAS (Figs. 2, 8, and Table VII). This means that the DCX can probe the change in nuclear structure as pairs of neutrons are changed into pairs of protons. Recent models of nuclear collective motion are based on the assumption that $J^\pi=0^+,2^+$ pairs of neutrons and protons are the most important degrees of freedom in the ground states of nuclei.[21–33] In these models nuclei which have only valence neutrons are predominantly spherical. As protons are added the nuclear system tends to a deformed structure. Hence the DCX will be probing this change in structure since it changes pairs of neutrons into protons.

In this paper we discussed only ${}_Z A(\pi^+,\pi^-){}_{Z+2}A$ DCX. Historically the reason for the emphasis on this reaction is because the DIAS transition was assumed to dominant. However, at low-pion energy (30–60 MeV) we have found in this paper that the transition to the ground state may be as large as to the double analog. This means that the ${}_{Z+2}A(\pi^-,\pi^+){}_Z A$ to the ground state may be large since it is the same as the ${}_Z A(\pi^+,\pi^-){}_Z A$ DCX to the ground state. Hence for the purposes of studying the relationship between the ground states of ${}_Z A$ and ${}_{Z+2}A$ either reaction will do, and in some cases (π^-,π^+) may be preferable.

This work was supported by the U.S. Department of Energy.

APPENDIX A

The two-nucleon cfp's can be generated from one-nucleon cfp's (Ref. 7) by the recursion relation

$$\langle j^n T,v=J=0\{\,|\,j^{n-2}\beta_1 T_1;j^2 T_2 J_2\rangle=\sqrt{2T_2+1}(-1)^{T_1+1+T}\times\sum_{T_3}\langle j^n T,v=J=0\{\,|\,j^{n-1}T_3\rangle\times\langle j^{n-1}T_3\{\,|\,j^{n-2}\beta_1 T_1 J_2\rangle\begin{Bmatrix}\frac{1}{2} & \frac{1}{2} & T_2\\ T_1 & T & T_3\end{Bmatrix}\sqrt{(2T_3+1)}\,, \tag{A1}$$

where for the $n-1$ system $v_3=1$ and $J_3=j$, and so these labels are omitted. The first cfp in the sum in (A1) is known analytically. The second is known analytically for the cases for which β_1 does not matter. For the cases in which β_1 does matter, the square root of the sum over the additional quantum number β_1 of the squared cfp is known analytically. In those cases we can determine analytically the square of the two-nucleon cfp summed over β_1. For the double analog transition $T'=T$ this does not matter because the cfp's come in exactly this combination as seen in (3.9). For the transition to the ground state $T'=T-2$, one needs to know a different product of cfp's. However, we can get around this by a sum rule. We know the matrix element of the isotensor operator $\hat{T}_-\hat{T}_-$ must vanish for such a transition. From this we derive that

$$\sum_{\substack{J_2 \text{ even}\neq 0\\ \beta_1}}\langle j^n T,v=J=0\{\,|\,j^{n-2}\beta_1 T_1;j^2 1,J_2\rangle\langle j^n T'=T-2,\ v=J=0\{\,|\,j^{n-1}\beta_1 T_1;j^2 1,J_2\rangle$$
$$=-\langle j^n T,v=J=0\{\,|\,j^{n-2}T_1;j^2 1,J_2=0\rangle\langle j^n T'=T-2,v=J=0\{\,|\,j^{n-2}T_1;j^2 1,J_2=0\rangle\,. \tag{A2}$$

Since there is no need for β_1 for seniority-zero states, the right-hand side of (A2) is well determined and is given in Table I.

APPENDIX B

In this appendix we shall derive the DCX amplitude in the neutron-proton basis of Ref. 20. The titanium eigenfunctions in this basis are given by (5.1). The calcium isotopes have only valence neutrons and hence have $v=J=0$ for the ground state. Since the DCX operator given in (2.2) changes two neutrons into two protons, we remove two neutrons from the calcium isotopes using the $T=n/2$ cfp's given in Table I, suppressing the unnecessary isospin and β labels:

$$F\left|j^n T=T_z=\frac{n}{2},J=0\right\rangle=-2\Omega\left[\frac{n(n-1)}{2}\right]^{1/2}\sum_{vJL}\langle j^n v=0\{\,|\,j^{n-2}vJ;j^2 J\rangle\begin{Bmatrix}j & j & L\\ j & j & J\end{Bmatrix}F_L\,|\,j^{n-2}vJ;j_\pi^2 J\rangle\,, \tag{B1}$$

where we have used (2.5) and the two nucleons coupled to angular momentum J are two protons. The factor under the square root counts the number of neutrons that can be converted into protons; the square root appears because an amplitude is involved. Taking the matrix element with (5.1) gives

$$\left\langle j^n T=T_z=\frac{n}{2}-2, J=0 \mid F \mid j^n T=T_z=\frac{n}{2}, J=0\right\rangle=-2\Omega \sum_{vJL} \begin{Bmatrix} j & j & L \\ j & j & J \end{Bmatrix} \langle j^n v=0\{ \mid j^{n-2} vJ; j^2 J\rangle \alpha(n; v, J) F_L \ . \tag{B2}$$

Comparing with (5.2a) this gives

$$\beta_L(n)=-2\Omega \Sigma_{vJ} \begin{Bmatrix} j & j & L \\ j & j & J \end{Bmatrix} \langle j^n v=0\{ \mid j^{n-2} vJ; j^2 J\rangle \alpha(n; v, J) \ . \tag{B3}$$

Getting the $T=n/2$, $T_1=n/2-1$ cfp's from Table I finally gives (5.2b). The negative sign of the $J>0$ cfp's is determined by requiring that the ground state have definite isospin, i.e., $\hat{T}_-$ operating on the ground state vanishes.

In Ref. 20 the eigenfunctions of ^{48}Cr were not calculated. However, the eigenfunction of the double analog of the ground state of ^{48}Ti, which occurs in ^{48}Cr, can be generated from the ground-state eigenfunction of ^{48}Ti by operating on this eigenfunction with $[4T(2T-1)]^{-1/2}\hat{T}_-\hat{T}_-$. By removing two neutrons via cfp's as described above, this operation can be carried out and leads to the wave function for the double analog in the neutron-proton basis given by

$$\left| j^n T=\frac{n}{2}-2, T_z=T-2, J=0\right\rangle=\Sigma_{v'vJ} \alpha'(n; v'vJ) \mid (j^4 v' J; j^{n-4} vJ)^{(0)}\rangle \ , \tag{B4}$$

where

$$\alpha'(n; v'vJ)=\left[\frac{6(n-2)(n-3)}{(n-4)(n-5)}\right]^{1/2} \Sigma_{12}(-1)^{J_1+J_2+J} \langle j^{n-2} v_1 J_1\{ \mid j^{n-4} vJ; j^2 J_2\rangle \langle j^4 v' J\{ \mid j^2 J_1; j^2 J_2\rangle \alpha(n; v_1 J_1) \ . \tag{B5}$$

Using this result, the DCX amplitude can be calculated in a similar manner as described above for the calcium isotopes yielding (5.3).

APPENDIX C

To test the effect on DCX of different models of the short-range behavior of the n-n system we insert a correlation factor

$$N[1-g(r)]^2 \equiv N[1-h(r)] \tag{C1}$$

into the initial n-n and final p-p density, i.e., N is determined numerically by the normalization condition

$$N \int \mid \psi(\mathbf{r}_2, \mathbf{r}_2) \mid^2 [1-g(r)]^2 d\mathbf{r}_1 d\mathbf{r}_2=1 \ . \tag{C2}$$

Strictly speaking, the correlated wave function is no longer of the form of the independent particle shell model (IPSM), but we will continue to use the coefficients of Table II as an approximation. Two forms of $g(r)$ have been chosen:

$$\text{hard sphere: } 1 \text{ if } r<r_c \text{ and } 0 \text{ if } r>r_c \ , \tag{C3a}$$

$$\text{Siegel: } 1-[1-\exp(-2.83r^2)(1-8r^2)]^{1/2} \ . \tag{C3b}$$

Correlation function (C3b) simulates short-range repulsion combined with intermediate-range attraction.

The correlation factor is included in the expression for F_L [Eq. (2.3)]. The term corresponding to "1" in the correlation factor is identical to the previous IPSM result. The term corresponding to $h(\mid \mathbf{r}_1-\mathbf{r}_2 \mid)$ is more difficult to evaluate because then r_1 and r_2 integrals no longer separate. The integral in Eq. (2.3) is nine-dimensional. We first transform $h(\mid \bar{r}_1-\bar{r}_2 \mid)$ to momentum space to get

$$\int d\mathbf{r}_1 \int d\mathbf{r}_2 \int d\mathbf{q} \int d\mathbf{q}' S(\mathbf{k}', \mathbf{k}, \mathbf{q}) e^{i\mathbf{r}_1\cdot(\mathbf{k}-\mathbf{q})} e^{i\mathbf{r}_1\cdot(\mathbf{q}-\mathbf{k}')} e^{-i\mathbf{q}'\cdot(\mathbf{r}_1-\mathbf{r}_2)} h(q') Y_{LM}(\hat{\mathbf{r}}_1) Y^*_{LM}(\hat{\mathbf{r}}_2) \psi^2(r_1) \psi^2(r_2)/(2\pi)^3 \ , \tag{C4}$$

where

$$S(\mathbf{k}, \mathbf{k}', \mathbf{q})=f(\mathbf{k}', \mathbf{q}) f(\mathbf{q}, \mathbf{k})/(q_0^2-k^2+i\epsilon) \ . \tag{C5}$$

The integrals over r_1 lead to

$$\int d\mathbf{r}_1 e^{i\mathbf{r}_1\cdot(\mathbf{k}-\mathbf{q}-\mathbf{q}')} \psi^2(r_1) Y_{LM}(\hat{\mathbf{r}}_1)=4\pi i^L \int j_L(\mid \mathbf{k}-\mathbf{q}-\mathbf{q}' \mid r_1) \psi^2(r_1) r_1^2 \, dr_1 \ \ Y_{LM}(\hat{\mathbf{r}}) \tag{C6}$$

where $\hat{\mathbf{r}}=(\mathbf{k}-\mathbf{q}-\mathbf{q}')/\mid \mathbf{k}-\mathbf{q}-\mathbf{q}' \mid$. The integral over r_2 is similar. Summing on M and setting

$$\mathbf{s}=-\mathbf{q}+(\mathbf{k}+\mathbf{k}')/2-\mathbf{q}=-\mathbf{q}'+\mathbf{u} \quad \text{and} \quad \mathbf{K}=(\mathbf{k}'-\mathbf{k})/2 ,$$

we find

$$\frac{(2L+1)}{2\pi^2}\int d\mathbf{q}\int d\mathbf{s}\, H_L(|\mathbf{K}-\mathbf{s}|)H_L(|\mathbf{K}+\mathbf{s}|)h(|\mathbf{u}-\mathbf{s}|)P_L(\omega)S(\mathbf{k}',\mathbf{k},\mathbf{q}) , \tag{C7}$$

where ω is the cosine of the angle between $\mathbf{K}+\mathbf{s}$ and $\mathbf{K}-\mathbf{s}$. It is convenient to define $B_L(K,s,\hat{\mathbf{K}}\cdot\hat{\mathbf{s}})=H_L H_L P_L$. Note that B_L is independent of angle if $K=0$ or if either $s \ll K$ or $s \gg K$. Thus we expect (and confirm in practice) that a Legendre expansion of the form

$$B_L=\Sigma_{lm} b_l^L(K,s)Y_{lm}^*(\hat{\mathbf{K}})Y_{lm}(\hat{\mathbf{s}}) \tag{C8}$$

will be rapidly convergent. The symmetry of B under $\bar{s}\rightarrow-\bar{s}$ implies that all odd-l terms in the expansion will vanish. Similarly we may expand

$$g(|\mathbf{u}-\mathbf{s}|)=\Sigma_{lm} g_l(\mathbf{u},\mathbf{s})Y_{lm}^*(\hat{\mathbf{s}})Y_{lm}(\hat{\mathbf{u}}) . \tag{C9}$$

The angular integration over $\bar{s}$ is then trivial, but the radial integration must be done numerically. If the axis of the $\mathbf{q}$ integration is taken along $(\mathbf{k}+\mathbf{k}')/2$ the integration about the axis can be done analytically, but the two remaining components of $\mathbf{q}$ must be integrated numerically. The principal value portion of the integral is evaluated by a subtraction procedure.

Cross sections for calcium isotopes calculated with a hard-sphere radius $r_c=0.6$ fm are given in Fig. 4(a). These results may be compared directly with those shown in Fig. 2, for which $r_c=0$ fm. Of particular note is the suppression of the ^{42}Ca (DIAS) and the ^{48}Ca (g.s.) transitions by roughly a factor of 2. In both of these processes the cross section is dominated by B, which we have seen (Fig. 3) is in turn largely dominated by the DCX on close neutron pairs. The analog transition on ^{48}Ca is less affected (especially at lower energy) because the B is suppressed by the factor $\frac{1}{7}$, and A is less sensitive to short-range correlations. Figure 4(b) shows the effect of intermediate-range attractive interactions between valence neutrons. The correlation function is taken from the thesis of Siegel.[40] The ^{42}Ca (DIAS) and ^{48}Ca (g.s.) transitions are seen to be increased by roughly a factor of 2.

*Permanent address: Tel Aviv University, Tel Aviv, Israel.

[1]G. A. Miller, Phys. Rev. C **24**, 221 (1981).

[2]E. R. Siciliano, M. D. Cooper, M. B. Johnson, and M. J. Leitch, Phys. Rev. C **34**, 267 (1986).

[3]W. R. Gibbs, W. B. Kaufmann, and P. B. Siegel, Proceedings of LAMPF Workshop on Pion Double Charge Exchange, edited by H. Baer and M. Leitch, Report No. LA-10550-C, 1985, p. 90.

[4]T. Karapiperas and M. Kobayashi, Phys. Rev. Lett. **54**, 1230 (1985).

[5]K. K. Seth *et al.*, Phys. Lett. **155B**, 339 (1985).

[6]Z. Weinfeld *et al.*, Phys. Rev. C **37**, 902 (1988).

[7]A. deShalit and I. Talmi, *Nuclear Shell Theory* (Academic, New York, 1963).

[8]D. H. Gloeckner and F. J. D. Serduke, Nucl. Phys. **A220**, 447 (1974).

[9]I. Talmi, Nucl. Phys. **A423**, 189 (1984).

[10]N. Auerbach, W. R. Gibbs, and E. Piasetzky, Phys. Rev. Lett. **59**, 1076 (1987).

[11]W. R. Gibbs, A. T. Hess, and W. B. Kaufmann, Phys. Rev. C **13**, 1982 (1976).

[12]T.-S. H. Lee, D. Kurath, and B. Zeidman, Phys. Rev. Lett. **39**, 1307 (1977).

[13]M. Bleszynski and R. J. Glauber, Phys. Rev. C **36**, 681 (1987).

[14]J. N. Ginocchio, Nucl. Phys. **63**, 449 (1965).

[15]A. K. Kerman, Ann. Phys. (N.Y.) **12**, 300 (1961); A. K. Kerman, R. D. Lawson, and M. M. Macfarlane, Phys. Rev. **124**, 162 (1961).

[16]I. Talmi, Nucl. Phys. **A172**, 1 (1971).

[17]J. N. Ginocchio and J. B. French, Phys. Lett. **7**, 137 (1963).

[18]J. D. McCullen, B. Bayman, and L. Zamick, Phys. Rev. B **134**, 515 (1964).

[19]J. N. Ginocchio, Phys. Rev. **144**, 952 (1966).

[20]J. D. McCullen, B. F. Bayman, and L. Zamick, Princeton University Technical Report No. NYO-9891, 1964 (unpublished); for ^{48}Ti this report treats the neutrons as holes while we use a phase convention consistent with treating the neutrons as particles.

[21]A. Arima and F. Iachello, *Advances in Nuclear Physics*, edited by J. W. Negele and E. Vogt (Plenum, New York, 1984), Vol. 13, p. 139.

[22]J. N. Ginocchio, Ann. Phys. (N.Y.) **126**, 234 (1980).

[23]C. L. Wu *et al.*, Phys. Lett. **168B**, 313 (1986).

[24]D. A. Sparrow and A. S. Rosenthal, Phys. Rev. C **18**, 1753 (1978).

[25]P. B. Siegel and W. R. Gibbs, Phys. Rev. C **33**, 1407 (1986).

[26]G. Rowe, M. Salomon, and R. H. Landau, Phys. Rev. C **18**, 584 (1978).

[27]H. W. Baer *et al.*, Phys. Rev. C **35**, 1425 (1987).

[28]E. Oset, D. Strottman, M. J. Vicente-Vacas, and M. Wei-Hsing, Nucl. Phys. **A408**, 461 (1983). We have corrected a misprint ($-k-k'$ should be $k-k'$) in the original Eq. (7). We have also included an additional factor of 2 as advised by D. Strottman.

[29]J. D. Zumbro *et al.*, Phys. Rev. C **36**, 1479 (1987).

[30]M. Kaletka *et al.*, Phys. Lett. **B199**, 336 (1987).

[31]M. Johnson, Phys. Rev. C **22**, 192 (1980).

[32]J. Alster and J. Warszawski, Phys. Rep. **52**, 87 (1979).

[33]J. Warszawski and N. Auerbach, Nucl. Phys. **276**, 402 (1977).

[34]N. Auerbach, Nucl. Phys. **76**, 321 (1966).

[35]N. Auerbach, Phys. Rev. **163**, 1203 (1967).

[36]T. Otsuka and A. Arima, Phys. Lett. **77B**, 1 (1978).

[37]B. Lorazo, Ann. Phys. (N.Y.) **92**, 95 (1975); see also O. Bohigas, C. Quesne, and R. Arvieu, Phys. Lett. **26B**, 562 (1968).

[38]M. J. Leitch *et al.*, Report No. LA-UR, 1988 (unpublished).

[39]G. E. Miller, Phys. Rev. Lett. **53**, 2008 (1984).

[40]P. B. Siegel, Ph.D. thesis, Arizona State University, 1986.